Journal of Engineering Mathematics **41:** 367–400, 2001.

Vorticity and the theory of aerodynamic sound

M. S. HOWE
Boston University, College of Engineering 110 Cummington Street, Boston MA 02215n U.S.A.
e-mail: mshowe@bu.edu

Received 13 December 2000; accepted in revised form 3 July 2001

Abstract. Lighthill strongly advocated the use of vortex methods in most areas of fluid mechanics with the notable exception of the theory of aerodynamic sound. But it is straightforward to transform his famous 'acoustic analogy' to make vorticity rather than Reynolds stress the ultimate 'source' of sound in homentropic flows. 'Vortex sound' theory becomes especially useful in applications involving acoustically *compact* flow-structure interactions, where it actually emerges as an extension of Kelvin's theory of 'vortex impulse', a notion that Lighthill regarded as important enough to be given special treatment in undergraduate lectures on fluid mechanics. The 'impulse source' can be recast in a form more suited for numerical or analytical evaluation, and is closely related to the 'compact Green's function'. Convergence difficulties encountered in the casual application of the acoustic analogy to non-compact flow-structure interactions are resolved in a natural manner by the methods of vortex sound theory. New illustrations of these methods are given in this paper by consideration of the unsteady development of lift by a starting airfoil, of the production of sound by a 'vortex whistle', and of the *infrasound* generated when a high-speed train enters the tunnel.

Key words: compact Green's function, high-speed train, Kirchhoff vector, vortex impulse, vortex sound, vortex-whistle

1. Introduction

James Lighthill possessed an encyclopedic knowledge of classical fluid mechanics and must have been well aware of Kelvin's [1] definition of a vortex in a homogeneous fluid, and of its significance for acoustics:

> *. . . a portion of fluid having any motion that it could not acquire by fluid pressure transmitted through itself from its boundary.*

In his famous introductory chapters to *Laminar Boundary Layers* [2], Lighthill was the first to recognize vorticity as the variable of paramount importance for the numerical calculation of incompressible flow past a solid surface. Methods based on the pressure or a stream function are 'inadequate'; the pressure, for example, 'involves solving an equation of Poisson's type in the whole infinite flow field, instead of in the region of nonzero vorticity, which includes only those portions of the fluid that have passed near the body surface.' Furthermore, 'fluid velocities respond by large sudden changes to any sudden alteration in the velocity or angular velocity of the solid surfaces, while pressures have enormous peaks (the so-called 'impulsive pressures') during such changes; on the other hand, the vorticity distribution varies smoothly,' being the only quantity whose variations are not propagated at the speed of sound. Once the vorticity has been determined the flow can be calculated everywhere.

Let $f(\mathbf{x}, t) = 0$ denote a control surface that 'moves with the fluid' and just encloses a solid surface S, with $f \gtrless 0$ respectively in the fluid and within the solid (see Figure 1). The

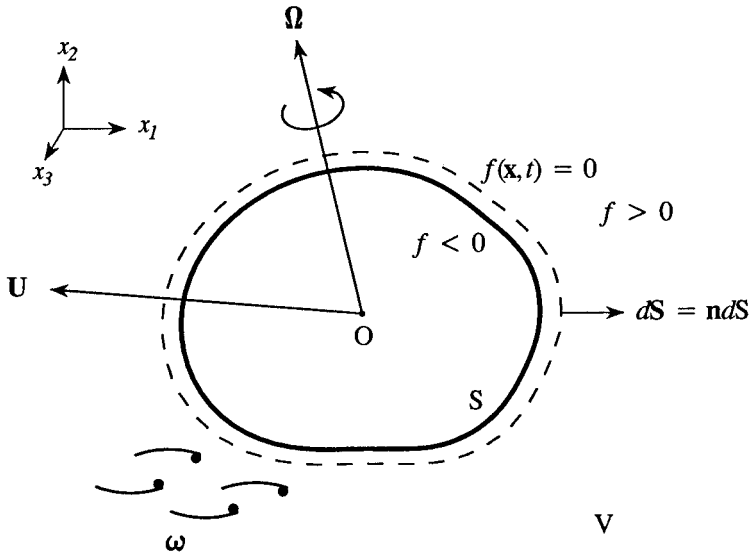

Figure 1. The control surface $f(\mathbf{x}, t) = 0$ that just encloses the surface S of a translating and rotating rigid body; V is the region $f(\mathbf{x}, t) > 0$ occupied by the fluid.

Heaviside step function $\mathrm{H}(f) = 1,\ 0$ according as $\mathbf{x}$ is without or within S at time t, and satisfies

$$\frac{\mathrm{DH}}{\mathrm{D}t} \equiv \frac{\partial \mathrm{H}}{\partial t} + \mathbf{v} \cdot \nabla \mathrm{H} = 0, \tag{1.1}$$

where $\mathbf{v}$ is the fluid velocity.

By multiplying the vorticity equation for incompressible flow by $\mathrm{H} \equiv \mathrm{H}(f)$ and rearranging, we find

$$\frac{\mathrm{D}}{\mathrm{D}t}(\mathrm{H}\boldsymbol{\omega}) - (\mathrm{H}\boldsymbol{\omega} \cdot \nabla)\mathbf{v} - \nu\nabla^2(\mathrm{H}\boldsymbol{\omega}) = -\nu\nabla(\nabla \mathrm{H} \cdot \boldsymbol{\omega}) + \nu \mathrm{curl}\ (\nabla \mathrm{H} \wedge \boldsymbol{\omega}) + \nu \nabla \mathrm{H} \wedge \mathrm{curl}\,\boldsymbol{\omega}, \tag{1.2}$$

where $\boldsymbol{\omega} = \mathrm{curl}\,\mathbf{v}$ is the vorticity and ν is the kinematic viscosity. The 'source' terms on the right-hand side involve $\nabla \mathrm{H} = \delta(f)\nabla f$, and are confined to the surface S, where the vector $\nabla \mathrm{H}$ is parallel to the unit normal $\mathbf{n}$ directed into the fluid; they are determined by the values of $\boldsymbol{\omega}$ and $\mathrm{curl}\,\boldsymbol{\omega}$ on S. The normal component of vorticity $\omega_n \equiv 2\mathbf{n} \cdot \boldsymbol{\Omega}$ on S if the body rotates with angular velocity $\boldsymbol{\Omega}$. Thus, to solve (1.2) we actually need to know $\boldsymbol{\omega}$ and the normal derivative of the *tangential* vorticity on S, because the solenoidality condition $\mathrm{div}\,\boldsymbol{\omega} = 0$ permits the normal derivative of the normal component of vorticity to be determined in terms of these quantities. But these quantities cannot be specified independently. For example, the final source on the right-hand side involves the viscous shear force $-\nu\mathrm{curl}\,\boldsymbol{\omega}$ on S, which can be 'determined' from the momentum equation in the form

$$-\nu\mathrm{curl}\,\boldsymbol{\omega} = \frac{\mathrm{D}\mathbf{U}}{\mathrm{D}t} + \frac{1}{\rho_o}\nabla p, \tag{1.3}$$

where $\mathbf{U}$ is the surface velocity, p is the pressure, and ρ_o the fluid density. This source of vorticity is independent of the viscosity. When it is given the remaining source term $\nabla \mathrm{H} \wedge \boldsymbol{\omega}$ is not arbitrary, but must be adjusted in value to ensure that $\mathrm{H}\boldsymbol{\omega}$ vanishes in the region $f < 0$.

Lighthill proposed a two-step method of solution that is the basis of many modern numerical schemes [3, 4]: at the beginning of the nth step of the calculation, at time t_n, say, the production of vorticity is ignored, and the existing distribution of vorticity is convected inviscidly over a small time interval until time $t_{n+\frac{1}{2}}$ with velocity determined by the Biot-Savart induction formula

$$\mathbf{v}(\mathbf{x}, t) = \text{curl} \int \frac{\boldsymbol{\omega}(\mathbf{y}, t)\mathrm{d}^3\mathbf{y}}{4\pi|\mathbf{x} - \mathbf{y}|}, \tag{1.4}$$

applied at $t = t_n$, where the integration is over the whole of space where $\boldsymbol{\omega} \neq \mathbf{0}$. In the case of a rotating boundary this formula would be applied with $\boldsymbol{\omega}(\mathbf{y}, t) = 2\boldsymbol{\Omega}$ for points $\mathbf{y}$ within S. The resulting velocity field is then augmented by an irrotational velocity distribution that ensures that the normal component of the velocity on S at time $t_{n+\frac{1}{2}}$ is equal to that of the solid.

The no-slip condition requires that the tangential velocities of the fluid and solid should also be equal on S. Let the calculated relative velocity at time $t_{n+\frac{1}{2}}$ be denoted by $\mathbf{v}_S(\mathbf{x}, t_{n+\frac{1}{2}})$. The amount of 'slip' determines the strength $\mathbf{n} \wedge \mathbf{v}_S(\mathbf{x}, t_{n+\frac{1}{2}})$ of the surface vorticity that must be generated and diffused into the flow during the remaining small time interval from $t_{n+\frac{1}{2}}$ to t_{n+1}. The diffusion takes place close to the boundary, where nonlinear convection can be ignored. In this region Equation (1.2) is approximated by linearizing the left-hand side, which then becomes a diffusion equation with surface sources. For example, for a stationary, plane boundary at $x_3 = 0$, the source $\nabla\mathrm{H}\cdot\boldsymbol{\omega} \equiv \mathbf{0}$, and the final term on the right of (1.2) (proportional to the surface drag force) vanishes for $t_{n+\frac{1}{2}} < t < t_{n+1}$. The surface source $\nu\,\text{curl}\,(\nabla\mathrm{H} \wedge \boldsymbol{\omega})$ adjusts itself to ensure that vorticity from the sheet does not diffuse into the wall, such that at time t_{n+1} the vorticity diffused from the boundary into the fluid (in $x_3 > 0$) is given by

$$\boldsymbol{\omega} = \frac{1}{4(\pi\nu\Delta t)^{\frac{3}{2}}} \iint_{-\infty}^{\infty} \mathbf{n} \wedge \mathbf{v}_S(y_1, y_2, t_{n+\frac{1}{2}}) \exp\left[-\frac{(x_1 - y_1)^2 + (x_2 - y_2)^2 + x_3^2}{4\nu\Delta t}\right] \mathrm{d}y_1\,\mathrm{d}y_2 \tag{1.5}$$

where $\Delta t = t_{n+1} - t_{n+\frac{1}{2}}$. Having determined the new vorticity we can proceed to the next step of the calculation.

Thus Lighthill concludes that 'any flow development is in principle computable by studying the diffusion of vortex lines, and their convection and stretching by the associated flow, while supposing normal and tangential vorticity to appear at the surface continuously, in just such measure as is required to maintain, respectively, the solenoidality of the vorticity field and the no-slip condition'.

When there are no solid boundaries, and the fluid is at rest at infinity, unsteady motion can persist only by virtue of the presence of vorticity. When the fluid is compressible part of the kinetic energy of the vortex field radiates away as sound. However, for twenty years or more, following the appearance of his monumental paper on aerodynamic sound [5], Lighthill accorded no public acknowledgment of the fundamental role of vorticity in the production of aerodynamic sound (the 'self noise' of a flow), although he had unambiguously identified the sound source at low Mach number with the essentially incompressible turbulence Reynolds stress whose evolution and fluctuations are governed by those of the vorticity. He argued that most unsteady flows of technological interest are of high Reynolds number and turbulent, and that the acoustic radiation is a very small by-product of the motion. Although turbulence is usually produced by fluid motion relative to solid boundaries or by the instability of free shear

layers separating a high-speed flow from a stationary environment, the influence of boundaries on the production of sound (by a jet, say), as opposed to the production of vorticity, could be ignored. The aerodynamic sound problem was thereby reduced to the study of the mechanism that converts kinetic energy of rotational motions into acoustic waves involving longitudinal vibrations of fluid particles. Lighthill solved this problem without specific reference to the underlying vortex field. In a fluid of uniform mean density he showed that the principal source type is a 'quadrupole' whose strength per unit volume is the Reynolds stress $\rho v_i v_j$.

By an inspired transformation of the exact equations of motion of a compressible fluid, Lighthill deduced an exact analogy between the production of sound by turbulence in a fluid whose mean pressure, density and sound speed are respectively p_o, ρ_o and c_o at large distances from the source flow, and that produced in an ideal, stationary acoustic medium (of mean pressure, density and sound speed equal p_o, ρ_o and c_o, respectively) forced by the stress distribution

$$T_{ij} = \rho v_i v_j + \big((p - p_o) - c_o^2(\rho - \rho_o)\big)\,\delta_{ij} - \sigma_{ij}, \tag{1.6}$$

where σ_{ij} is the viscous stress. T_{ij} is called the *Lighthill stress tensor*, and is equal to the quadrupole source strength in Lighthill's equation

$$\left(\frac{1}{c_o^2}\frac{\partial^2}{\partial t^2} - \nabla^2\right)[c_o^2(\rho - \rho_o)] = \frac{\partial^2 T_{ij}}{\partial x_i \partial x_j}. \tag{1.7}$$

This equation formally describes the production of fluctuations in $c_o^2(\rho - \rho_o)$ by the stress distribution $T_{ij}(\mathbf{x}, t)$. The disturbances propagate as sound waves away from the source region, and in the distant field where the background flow is quiescent and flow perturbations may be regarded as small, the acoustic pressure $p(\mathbf{x}, t) - p_o \equiv c_o^2(\rho - \rho_o)$.

However, Lighthill's Equation (1.7) is merely a *rearrangement* of the Navier-Stokes equation (in combination with the continuity equation) that supplies a useful representation of sound generation only when T_{ij} is known. T_{ij} strictly accounts not only for the production of sound by the flow, but also for nonlinear self-modulation of the sound, for convection, scattering and refraction by flow velocity and sound speed variations, and for attenuation due to thermal and viscous actions. In many applications nonlinear effects are sufficiently weak to be neglected within the source region, although they may affect propagation to a distant observer. Convection and refraction of sound within and near the source flow can be important, for example when the sources are contained in a turbulent shear layer, or are adjacent to a large, quiescent region of fluid whose mean thermodynamic properties differ from those in the radiation zone; such effects are governed by contributions to T_{ij} that are *linear* in the perturbation quantities relative to a mean background flow. Thus, the utility of Lighthill's equation rests on the hypothesis that all of these effects can be ignored, or can somehow be determined and explicitly included in T_{ij}, either analytically [6–8] or using data derived from an accurate numerical simulation of the unsteady *compressible* motions in the source region. When this is not possible predictions based on Lighthill's equation are strictly valid only when the characteristic Mach number M of the source flow satisfies $M^2 \ll 1$, although the equation has frequently been applied to high speed flows with apparent success.

It turns out [9, Section 2.3] that, in order to cast Lighthill's equation in a form that brings vorticity to the fore as the ultimate source of sound (being the one property of the flow that always varies smoothly, and 'the only quantity whose variations are not propagated at the enormous speed of sound'), it is necessary to adopt the *total enthalpy* B rather than $c_o^2(\rho - \rho_o)$

as the acoustic variable. The source terms in the reformulated theory are then confined to those regions where the vorticity $\boldsymbol{\omega} \neq \mathbf{0}$ and where $\nabla s \neq \mathbf{0}$, where s is the entropy. In many applications (for example, in the absence of combustion, and when the Mach number is small enough for the mean density to be regarded as uniform) it is permissible to regard the source flow as *homentropic*. Lighthill's equation then assumes the form

$$\left(\frac{\mathrm{D}}{\mathrm{D}t}\left(\frac{1}{c^2}\frac{\mathrm{D}}{\mathrm{D}t}\right) - \frac{1}{\rho}\nabla\cdot(\rho\nabla)\right) B = \frac{1}{\rho}\mathrm{div}(\rho\boldsymbol{\omega}\wedge\mathbf{v}), \tag{1.8}$$

where Bernoulli's equation implies that in the absence of vorticity and moving boundaries the total enthalpy

$$B = \int \frac{\mathrm{d}p}{\rho} + \frac{1}{2}v^2 \tag{1.9}$$

is a constant that may be assumed to vanish.

Apart from the obvious difference in the acoustic source terms in Equations (1.7) and (1.8), the left-hand side of the vortex sound Equation (1.8) takes explicit account of nonlinear effects on propagation, because the local values of the density ρ, sound speed c and the flow velocity $\mathbf{v}$ all occur in the differential wave-operator. In an extensive region of turbulence, whose size exceeds many characteristic acoustic wavelengths, or where a mean shear layer contributes a large *linear* contribution to the fluctuating part of $\boldsymbol{\omega}\wedge\mathbf{v}$, scattering and refraction within the source region can still be important, and is implicitly included in the source term of Equation (1.8). Outside the source flow the unsteady motion is entirely irrotational with velocity potential $\varphi(\mathbf{x}, t)$, say, and $B = -\partial\varphi/\partial t$, so that B is easily related to the acoustic pressure in the far field (when the fluid is at rest at infinity $p - p_o = \rho_o B$).

In Sections 2 and 3 of this paper we shall discuss the relation between the two forms (1.7) and (1.8) of Lighthill's acoustic analogy with particular reference to the influence of the presence of compact and non-compact solid bodies on sound production. This will lead to a consideration of the *impulse* of the source region, which can be expressed in terms of the so-called Kirchhoff vector of the solid, and to the useful concept of 'compact Green's function'. In the final Section 4 illustrative applications of vortex methods are made to study the development of lift by a starting airfoil, sound generation by a vortex whistle, and the very low frequency sound produced when a high-speed train enters a tunnel.

2. Vortex sound and impulse

2.1. Vorticity and the velocity quadrupole

There is no particular virtue in adopting vorticity as opposed to Reynolds stress as the effective source of the sound produced by turbulence in a nominally unbounded fluid. Dynamic variations in the mean density in the source region can be neglected when the turbulence Mach number is small, and if the motion is regarded as homentropic we may suppose that $p - p_o = c_o^2(\rho - \rho_o)$ (to within an error $\sim O(\rho_o v^2 M^2)$, where $M = v/c_o$), so that T_{ij} becomes equal to the *velocity* quadrupole source of strength $\rho_o v_i v_j$ when viscous stresses are neglected. Henceforth we shall denote the local value of the *perturbation* pressure $p - p_o$ by $p(\mathbf{x}, t)$, and take the coordinate origin at some convenient point in the source region, in which case the solution of Lighthill's Equation (1.7) in an unbounded fluid becomes

$$p(\mathbf{x},t) = \frac{\partial^2}{\partial x_i \partial x_j}\int \frac{\rho_o v_i v_j(\mathbf{y}, t-|\mathbf{x}-\mathbf{y}|/c_o)}{4\pi|\mathbf{x}-\mathbf{y}|}\,\mathrm{d}^3\mathbf{y}$$
$$\approx \frac{x_i x_j}{4\pi c_o^2|\mathbf{x}|^3}\frac{\partial^2}{\partial t^2}\int \rho_o v_i v_j(\mathbf{y}, t-|\mathbf{x}-\mathbf{y}|/c_o)\,\mathrm{d}^3\mathbf{y}, \quad |\mathbf{x}|\to\infty. \tag{2.1}$$

Let us apply this formula to a region of turbulence consisting of 'eddies' of correlation length ℓ and velocity v (Figure 2a). The characteristic frequency of the sources is therefore $\partial/\partial t \sim v/\ell$, and the wavelength of the sound they produce $\sim \ell/M \gg \ell$. Each eddy is said to be acoustically *compact*, and one easily deduces [3], [9, Section 2.1], [10], [11] that the order of magnitude of the pressure radiated by a *single* eddy $p(\mathbf{x},t) \sim (\ell/|\mathbf{x}|)\rho_o v^2 M^2$, and that the acoustic power $\sim 4\pi|\mathbf{x}|^2 p^2/\rho_o c_o \approx \ell^2\rho_o v^8/c_o^5 = \ell^2\rho_o v^3 M^5$. This is Lighthill's v^8-law. Because energy must be supplied at a rate $\sim \ell^2\rho_o v^3$ (per eddy) to maintain the flow, it shows also that only a minute fraction $\sim O(M^5)$ of the available kinetic energy of the flow is radiated as sound.

The radiation can be expressed in terms of the vorticity by noting that the source flow velocity v_i may be regarded as incompressible when M is small, and therefore that

$$\frac{\partial^2(v_i v_j)}{\partial x_i \partial x_j} = \mathrm{div}\,(\boldsymbol{\omega}\wedge\mathbf{v}) + \nabla^2(\tfrac{1}{2}v^2).$$

Equation (2.1) becomes

$$p(\mathbf{x},t) \approx \frac{-x_i}{4\pi c_o|\mathbf{x}|^2}\frac{\partial}{\partial t}\int \rho_o(\boldsymbol{\omega}\wedge\mathbf{v})_i(\mathbf{y}, t-|\mathbf{x}-\mathbf{y}|/c_o)\,\mathrm{d}^3\mathbf{y}$$
$$+ \frac{1}{4\pi c_o^2|\mathbf{x}|}\frac{\partial^2}{\partial t^2}\int \frac{1}{2}\rho_o v^2(\mathbf{y}, t-|\mathbf{x}-\mathbf{y}|/c_o)\,\mathrm{d}^3\mathbf{y}, \quad |\mathbf{x}|\to\infty, \tag{2.2}$$

When this is applied to a single turbulent eddy, retarded time differences can be neglected in the second integral ($t-|\mathbf{x}-\mathbf{y}|/c_o \approx t-|\mathbf{x}|/c_o$), which therefore is just equal to the retarded value of the kinetic energy of the eddy. It is then easy to deduce [9, Section 2.1], [12, Section 1.13] that the order of magnitude of the second term on the right of (2.2) is equal to the larger of

$$\frac{\ell}{|\mathbf{x}|}\rho_o v^2 M^4 \qquad \text{and} \qquad \frac{\ell}{|\mathbf{x}|}\frac{\rho_o v^2 M^2}{\mathrm{Re}}, \tag{2.3}$$

where $\mathrm{Re} = v\ell/\nu \gg 1$ is the Reynolds number. These correspond respectively to estimates of eddy dissipation caused by acoustic radiation damping and viscous losses.

It is not permissible to neglect retarded time differences across the eddy when estimating the value of the first integral on the right of (2.2), because $\int(\boldsymbol{\omega}\wedge\mathbf{v})(\mathbf{y},t)\mathrm{d}^3\mathbf{y} \equiv \mathbf{0}$. Thus, observing that $|\mathbf{x}-\mathbf{y}| \approx |\mathbf{x}| - \mathbf{x}\cdot\mathbf{y}/|\mathbf{x}|$ when $|\mathbf{x}|\to\infty$, we expand the integrand in powers of the retarded time variation $\mathbf{x}\cdot\mathbf{y}/c_o|\mathbf{x}|$. The first term in the expansion yields,

$$p(\mathbf{x},t) \approx \frac{-\rho_o x_i x_j}{4\pi c_o^2|\mathbf{x}|^3}\frac{\partial^2}{\partial t^2}\int y_i(\boldsymbol{\omega}\wedge\mathbf{v})_j(\mathbf{y}, t-|\mathbf{x}|/c_o)\,\mathrm{d}^3\mathbf{y} \quad \sim \frac{\ell}{|\mathbf{x}|}\rho_o v^2 M^2, \tag{2.4}$$

which is large compared with either of (2.3), but of exactly the same order as Lighthill's original estimate.

The dominant component of the Lighthill velocity quadrupole is therefore the vortex source $\mathrm{div}(\boldsymbol{\omega}\wedge\mathbf{v})$. The above argument is a refinement of one developed by Powell [13] in the

late 1950's. For many years Lighthill, the leading proponent of vortex methods, vigorously opposed Powell's theory [14].

2.2. Radiation from an acoustically compact solid in turbulent flow

The influence on sound production of a solid immersed in a turbulent flow at low Mach numbers is readily derived from the Ffowcs Williams - Hawkings equation [7] (which reduces to Curle's equation [15] when the body is stationary). To do this we introduce a control surface $f(\mathbf{x}, t) = 0$ that moves with the fluid and just encloses the surface S (as in Figure 1); where $f(\mathbf{x}, t) \gtrless 0$ respectively within the region V occupied by the fluid and within S. The momentum and continuity equations are multiplied by $\mathrm{H} \equiv \mathrm{H}(f)$ and combined to form the analogue of Lighthill's Equation (1.7) for the quantity $\mathrm{H}c_o^2(\rho - \rho_o)$:

$$\left(\frac{1}{c_o^2}\frac{\partial^2}{\partial t^2} - \nabla^2\right)[\mathrm{H}c_o^2(\rho - \rho_o)] = \frac{\partial^2(\mathrm{H}T_{ij})}{\partial x_i \partial x_j} - \frac{\partial}{\partial x_i}\left(p'_{ij}\frac{\partial \mathrm{H}}{\partial x_j}\right) + \frac{\partial}{\partial t}\left(\rho_o v_j \frac{\partial \mathrm{H}}{\partial x_j}\right), \qquad (2.5)$$

where

$$p'_{ij} = (p - p_o)\delta_{ij} - \sigma_{ij} \qquad (2.6)$$

is the compressive stress tensor.

Equation (2.5) is the differential *Ffowcs Williams - Hawkings* equation. It is valid throughout the whole of space, including the region within S (where $\mathrm{H}c_o^2(\rho - \rho_o) \equiv 0$). The presence of the body is represented by 'dipole' and 'monopole' source distributions concentrated on S, corresponding respectively to the second and third source terms on the right-hand side. The outgoing wave solution of (2.5) consists of waves diverging from these 'sources', so that in the approximation of low Mach number, homentropic flow (when $T_{ij} \approx \rho_o v_i v_j$) we obtain the following generalization of (2.1) [7]

$$\begin{aligned}\mathrm{H}c_o^2(\rho - \rho_o) \equiv\ \mathrm{H}p(\mathbf{x}, t) = \frac{\partial^2}{\partial x_i \partial x_j}\int_{\mathrm{V}(\tau)} \frac{[\rho_o v_i v_j]}{4\pi|\mathbf{x} - \mathbf{y}|}\,\mathrm{d}^3\mathbf{y} - \frac{\partial}{\partial x_i}\oint_{\mathrm{S}(\tau)} \frac{[p'_{ij}]}{4\pi|\mathbf{x} - \mathbf{y}|}\,\mathrm{dS}_j(\mathbf{y}) \\ + \frac{\partial}{\partial t}\oint_{\mathrm{S}(\tau)} \frac{[\rho_o v_j]}{4\pi|\mathbf{x} - \mathbf{y}|}\,\mathrm{dS}_j(\mathbf{y}) \qquad (2.7)\end{aligned}$$

where quantities in square brackets [ ] are evaluated at the retarded time $\tau = t - |\mathbf{x} - \mathbf{y}|/c_o$. The surface integrals are over the retarded surface $\mathrm{S}(\tau)$ defined by $f(\mathbf{x}, \tau) = 0$ (the surface element $\mathrm{dS}_j(\mathbf{y})$ being directed into the fluid), and the volume integral is over the region $\mathrm{V}(\tau)$ where $f(\mathbf{y}, \tau) > 0$ outside $\mathrm{S}(\tau)$. The radiation from the three source terms produces a null field within S (where $\mathrm{H} = 0$).

The first integral in (2.7) is the direct quadrupole radiation from the turbulence, and its order of magnitude at low Mach numbers $\sim (\ell/|\mathbf{x}|)\rho_o v^2 M^2$ per eddy, the same as for radiation into an unbounded medium. The first surface integral is the radiation from the dipoles on S. Its main contribution for a compact body (Figure 2b), whose diameter is comparable to the scale of the neighbouring turbulence, is obtained (for $|\mathbf{x}| \to \infty$) by neglecting retarded time variations over S. The strength of this source is

$$F_i(t) = \oint_{\mathrm{S}} p'_{ij}(\mathbf{y}, t)\,\mathrm{dS}_j(\mathbf{y}), \qquad (2.8)$$

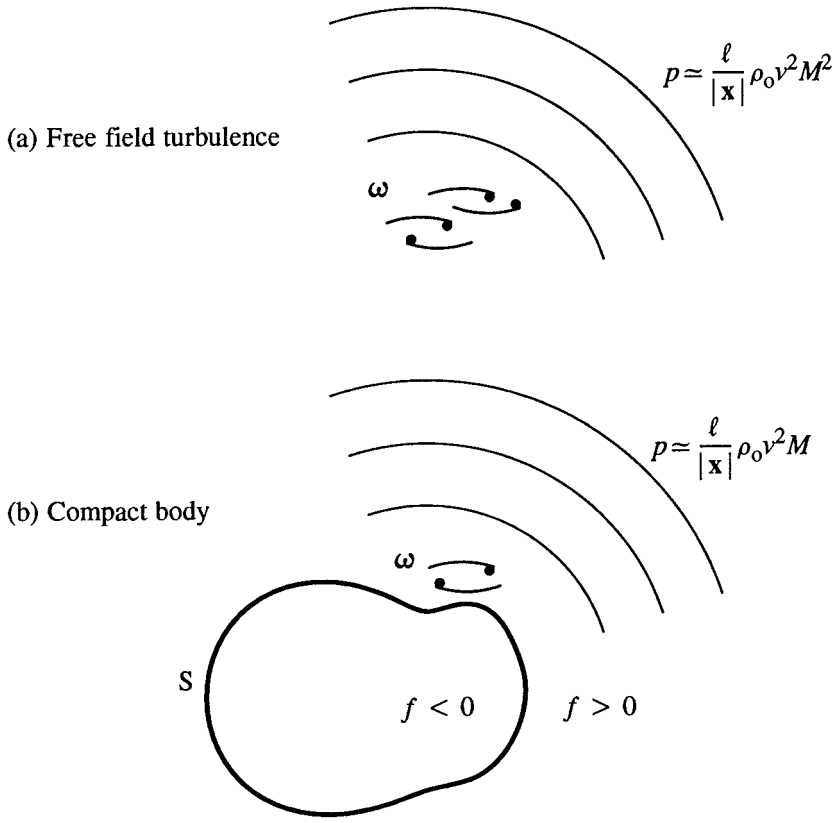

Figure 2. Sound generation by (a) free field vorticity and (b) vorticity in the vicinity of a compact rigid body in arbitrary motion.

which is just the net force exerted on the fluid by the rigid body, and may be evaluated by regarding the fluid as incompressible.

The final integral in (2.7) vanishes when retarded time variations are neglected on S, because the net volume outflow from a rigid surface is null. By expanding in powers of the retarded time element $\mathbf{x}\cdot\mathbf{y}/c_o|\mathbf{x}|$ one finds that its leading-order contribution is a *dipole* of strength $\rho_o\Delta\mathrm{d}\mathbf{U}/\mathrm{d}t$, where Δ is the volume enclosed by S and $\mathbf{U}(t)$ is the velocity of its centre of volume.

The overall dipole radiation can therefore be written

$$p(\mathbf{x},t) \approx \frac{x_i}{4\pi c_o|\mathbf{x}|^2}\frac{\partial}{\partial t}\left[F_i + \rho_o\Delta\frac{\mathrm{d}U_i}{\mathrm{d}t}\right]_{t-\frac{|\mathbf{x}|}{c_o}} \sim \frac{\ell}{|\mathbf{x}|}\rho_o v^2 M, \quad |\mathbf{x}| \to \infty, \tag{2.9}$$

which at small Mach numbers exceeds the quadrupole pressure by a factor of order $1/M$. Thus, the sound generated by a compact body in low Mach number turbulence is produced by a dipole whose strength is the net force that must be applied to the fluid-solid system when the mass density of the solid is taken to equal the mean density ρ_0 of the fluid.

The pressure distribution on S is governed in incompressible flow by a Poisson equation, and tends to be a diffuse quantity subject to large impulsive variations. The integral (2.8) determines F_i in terms of the pressure on S; but a knowledge of the distribution of unsteady surface pressure is often of no help when, for example, one is interested in modifying the

flow or surface geometry to minimize the production of dipole sound. According to Lighthill [2] pressure is precisely the quantity to avoid; a proper understanding of the *hydrodynamic* mechanisms controlling F_i must be sought in terms of the vorticity [16, 17].

However, provided the body is compact, the motion in the immediate neighbourhood of S can be regarded as incompressible, and the kinematic Biot-Savart induction formula (1.4) can be used to furnish just such a representation of the sound in terms of the vorticity for a body moving in an arbitrary fashion with angular velocity $\boldsymbol{\Omega}$. Indeed, it may be assumed that $\boldsymbol{\omega} = \mathbf{0}$ outside some bounded region enclosing S; and therefore that $\int \operatorname{div}\Big(y_i \boldsymbol{\omega}(\mathbf{y}, t)\Big)\mathrm{d}^3\mathbf{y} = 0$, $\int \operatorname{div}\Big(y_i y_j \boldsymbol{\omega}(\mathbf{y}, t)\Big)\mathrm{d}^3\mathbf{y} = 0$, where the integrations are over the whole of space, including the region occupied by the body, where $\boldsymbol{\omega} = 2\boldsymbol{\Omega}$. Then as $|\mathbf{x}| \to \infty$ (see [18], Sections 2.9, 7.3)

$$\int \frac{\boldsymbol{\omega}(\mathbf{y}, t)\mathrm{d}^3\mathbf{y}}{4\pi|\mathbf{x}-\mathbf{y}|} \sim \frac{1}{4\pi|\mathbf{x}|^3}\int (\mathbf{x}\cdot\mathbf{y})\boldsymbol{\omega}(\mathbf{y}, t)\mathrm{d}^3\mathbf{y} \equiv \nabla\left(\frac{1}{4\pi|\mathbf{x}|}\right) \wedge \frac{1}{2}\int \mathbf{y}\wedge\boldsymbol{\omega}(\mathbf{y}, t)\mathrm{d}^3\mathbf{y},$$

and therefore the representation (1.4) yields

$$\mathbf{v}(\mathbf{x}, t) \sim \operatorname{curl}\operatorname{curl}\left(\frac{\mathbf{G}(t)}{4\pi|\mathbf{x}|}\right) \equiv \nabla \operatorname{div}\left(\frac{\mathbf{G}(t)}{4\pi|\mathbf{x}|}\right), \quad |\mathbf{x}| \to \infty, \tag{2.10}$$

where the moment integral

$$\mathbf{G}(t) = \frac{1}{2}\int \mathbf{y}\wedge\boldsymbol{\omega}(\mathbf{y}, t)\mathrm{d}^3\mathbf{y}; \tag{2.11}$$

is the specific *impulse* of the fluid-solid system (the '**G**' notation is due to Lighthill [17], [19, Section 1.9]).

The incompressible motion in the irrotational region far from the body is therefore defined by $\varphi(\mathbf{x}, t) = \operatorname{div}(\mathbf{G}(t)/4\pi|\mathbf{x}|)$, which is the velocity potential of a hydrodynamic dipole that can be matched onto an outgoing acoustic dipole field that represents the sound produced by the fluid-solid interaction. This is done by replacing $\mathbf{G}(t)$ by $\mathbf{G}(t - |\mathbf{x}|/c_o)$ [20] [21, Section 7.4], [22, Section 6.4]. In the acoustic far field (where the undisturbed fluid is stationary) the pressure $p(\mathbf{x}, t) = -\rho_o \partial\varphi/\partial t$, and we therefore obtain the following representation of the sound in terms of the vorticity

$$p(\mathbf{x}, t) \approx \frac{\rho_o x_i}{4\pi c_o|\mathbf{x}|^2}\frac{\partial^2 G_i}{\partial t^2}\left(t - \frac{|\mathbf{x}|}{c_o}\right) = \frac{\rho_o x_i}{8\pi c_o|\mathbf{x}|^2}\frac{\partial^2}{\partial t^2}\int (\mathbf{y}\wedge\boldsymbol{\omega})_i \left(\mathbf{y}, t - \frac{|\mathbf{x}|}{c_o}\right)\mathrm{d}^3\mathbf{y}, \quad |\mathbf{x}| \to \infty. \tag{2.12}$$

The equivalence of this and the Ffowcs Williams - Hawkings result (2.9) can be deduced from the impulse formula of classical fluid mechanics, which supplies ([9], Section 1.14)

$$\mathbf{F} + \rho_o \Delta \frac{\mathrm{d}\mathbf{U}}{\mathrm{d}t} = \rho_o \frac{\mathrm{d}\mathbf{G}}{\mathrm{d}t} \equiv \frac{\rho_o}{2}\frac{\mathrm{d}}{\mathrm{d}t}\int \mathbf{y}\wedge\boldsymbol{\omega}(\mathbf{y}, t)\mathrm{d}^3\mathbf{y}. \tag{2.13}$$

The dipole strength $\mathrm{d}\mathbf{G}/\mathrm{d}t$ vanishes identically for compact turbulence in unbounded flow, when the acoustic source must actually be a much less efficient quadrupole. Möhring [23] showed that the radiation in this case (which is given by (2.4)) can be expressed in terms of a *second* moment of the vorticity. Take the cross product of $\mathbf{y}$ with the high-Reynolds-number vorticity equation $\partial\boldsymbol{\omega}/\partial t + \operatorname{curl}(\boldsymbol{\omega}\wedge\mathbf{v}) = 0$ (expressed in terms of $\mathbf{y}$ and t as independent variables), multiply by y_i, and use the identity

$$\mathbf{y} \wedge \operatorname{curl} \mathbf{A} = 2\mathbf{A} + \nabla(\mathbf{y} \cdot \mathbf{A}) - \frac{\partial}{\partial y_j}(y_j \mathbf{A}), \tag{2.14}$$

to deduce that the integral in (2.4) can be written

$$\int y_i(\boldsymbol{\omega} \wedge \mathbf{v})_j \mathrm{d}^3\mathbf{y} = -\frac{1}{3}\frac{\partial}{\partial t}\int y_i(\mathbf{y} \wedge \boldsymbol{\omega})_j \mathrm{d}^3\mathbf{y} + \frac{1}{3}\delta_{ij}\int \frac{1}{2}v^2 \mathrm{d}^3\mathbf{y}.$$

According to the estimates (2.3) the second integral on the right can be neglected, and expression (2.4) for the sound produced by turbulence in an unbounded flow then reduces to Möhring's form

$$p(\mathbf{x}, t) \approx \frac{\rho_o x_i x_j}{12\pi c_o^2 |\mathbf{x}|^3}\frac{\partial^3}{\partial t^3}\int [y_i(\mathbf{y} \wedge \boldsymbol{\omega})_j] \mathrm{d}^3\mathbf{y}, \quad |\mathbf{x}| \to \infty. \tag{2.15}$$

In applications the representation (2.12) of the sound generated by the flow-structure interaction is just as inconvenient as (2.9), since to evaluate the integral we must know $\boldsymbol{\omega}$ everywhere, including the region occupied by S. To be sure $\boldsymbol{\omega} = 2\boldsymbol{\Omega}$ within S for a body rotating with angular velocity Ω. But vorticity is also distributed on S, and its evolution is *not* governed by the equations of fluid mechanics. For example, it is often permissible to regard a rotational high-Reynolds-number flow as inviscid; the integral (2.12) would then include not only the free field vorticity, but also *bound vorticity* contained in the vortex sheet formed on the surface of the body by the 'slipping' of the inviscid fluid over S.

2.3. $\mathrm{d}\mathbf{G}/\mathrm{d}t$ EXPRESSED IN TERMS OF THE VORTEX FORCE $\boldsymbol{\omega} \wedge \mathbf{v}$

The integral representation of the time derivative $\mathrm{d}\mathbf{G}/\mathrm{d}t$ of the impulse integral (2.11) (which determines the surface force via (2.13)) can be transformed to remove the strong dependence of the integrand on the bound vorticity. This vorticity is produced both by motion of S and by relative motion between S and the fluid induced by the 'free' vorticity. Thus, any attempt to recast $\mathrm{d}\mathbf{G}/\mathrm{d}t$ is likely to be strongly influenced by the shape and velocity of motion of S; the following discussion is limited to the important special case in which S is in *translational* motion without rotation at velocity $\mathbf{U}(t)$.

Introduce the control surface $f(\mathbf{x}, t) = 0$ enclosing S, and the Heaviside function $\mathrm{H} \equiv \mathrm{H}(f)$ that satisfies (1.1). Multiply the momentum equation

$$\frac{\partial \mathbf{v}}{\partial t} + \nabla B = -\boldsymbol{\omega} \wedge \mathbf{v} - \nu \operatorname{curl} \boldsymbol{\omega} \tag{2.16}$$

by $\mathrm{H} \equiv \mathrm{H}(f)$, and take the curl of the resulting equation. Using (1.1) and the no-slip condition on S, we find

$$\begin{aligned}\frac{\partial}{\partial t}(\mathrm{H}\boldsymbol{\omega}) = & -\frac{\partial}{\partial t}(\nabla \mathrm{H} \wedge \mathbf{U}) - \operatorname{curl}\Big((\nabla \mathrm{H} \cdot \mathbf{U})\mathbf{U}\Big) - \nabla \mathrm{H} \wedge \nabla B - \operatorname{curl}(\mathrm{H}\boldsymbol{\omega} \wedge \mathbf{v}) \\ & - \nu \operatorname{curl}(\mathrm{H} \operatorname{curl} \boldsymbol{\omega}).\end{aligned} \tag{2.17}$$

Then, because $\boldsymbol{\omega} = \mathbf{0}$ within S, (2.11) yields

$$
\begin{aligned}
2\frac{\mathrm{d}\mathbf{G}}{\mathrm{d}t} &= \frac{\mathrm{d}}{\mathrm{d}t}\int \mathbf{y}\wedge(\mathrm{H}\boldsymbol{\omega})\mathrm{d}^3\mathbf{y} = \int \mathbf{y}\wedge\frac{\partial}{\partial t}(\mathrm{H}\boldsymbol{\omega})\mathrm{d}^3\mathbf{y} \\
&= -\int \mathbf{y}\wedge\frac{\partial}{\partial t}(\nabla\mathrm{H}\wedge\mathbf{U})\mathrm{d}^3\mathbf{y} - \int \mathbf{y}\wedge\mathrm{curl}\left((\nabla\mathrm{H}\cdot\mathbf{U})\mathbf{U}\right)\mathrm{d}^3\mathbf{y} - \int \mathbf{y}\wedge(\nabla\mathrm{H}\wedge\nabla B)\mathrm{d}^3\mathbf{y} \\
&\quad - \int \mathbf{y}\wedge\mathrm{curl}\,(\mathrm{H}\boldsymbol{\omega}\wedge\mathbf{v})\mathrm{d}^3\mathbf{y} - \nu\int \mathbf{y}\wedge\mathrm{curl}\,(\mathrm{H}\mathrm{curl}\,\boldsymbol{\omega})\mathrm{d}^3\mathbf{y} \\
&= 2\Delta\frac{\mathrm{d}\mathbf{U}}{\mathrm{d}t} + 0 + 2\oint_{\mathrm{S}} B\mathrm{d}\mathbf{S} - 2\int_V \boldsymbol{\omega}\wedge\mathbf{v}\mathrm{d}^3\mathbf{y} - 2\nu\oint_S \boldsymbol{\omega}\wedge\mathrm{d}\mathbf{S}, \qquad (2.18)
\end{aligned}
$$

where the last line follows from the identity (2.14) and the relation

$$\int(\,\cdot\,)\nabla\mathrm{H}\mathrm{d}^3\mathbf{y} = \oint_{\mathrm{S}}(\,\cdot\,)\mathrm{d}\mathbf{S},$$

the vector surface element $\mathrm{d}\mathbf{S}$ being directed into the fluid. Adopting the suffix notation we can re-write (2.18) in the form

$$\frac{\mathrm{d}G_i}{\mathrm{d}t} = \Delta\frac{\mathrm{d}U_i}{\mathrm{d}t} + \oint_{\mathrm{S}} Bn_i\mathrm{d}S - \int_{\mathrm{V}}\nabla y_i\cdot(\boldsymbol{\omega}\wedge\mathbf{v})\mathrm{d}^3\mathbf{y} - \nu\oint_{\mathrm{S}}\nabla y_i\cdot\boldsymbol{\omega}\wedge\mathrm{d}\mathbf{S}. \qquad (2.19)$$

The surface integral $\oint_{\mathrm{S}} Bn_i\mathrm{d}S$ can be eliminated by means of a procedure due to Kirchhoff (see [18], Section 6.4) involving the harmonic functions

$\varphi_i^*(\mathbf{y}) =$ the velocity potential of incompressible flow

produced by motion of S at unit speed in the i-direction.

(If S is multiply connected $\varphi_i^*(\mathbf{y})$ is defined as a single valued function by requiring the circulations about all irreducible contours to vanish. Also, $\varphi_i^*(\mathbf{y})$ is strictly a function of $\mathbf{y}-\mathbf{x}_{\mathrm{o}}(t)$ where $\mathbf{x}_{\mathrm{o}}(t)$ is the instantaneous position vector of the centre of volume of S; but it is convenient to suppress the dependence on t.) These potential functions are evidently a geometrical property of S, and satisfy

$$n_j\frac{\partial\varphi_i^*}{\partial y_j} = n_i \quad \text{on S,} \quad \text{and} \quad \nabla\varphi_i^* \sim O\left(\frac{1}{|\mathbf{y}|^3}\right) \quad \text{as} \quad |\mathbf{y}|\to\infty.$$

They usually arise in connection with the *added mass* tensor ([18], Section 6.4)

$$M_{ij} = M_{ji} = -\rho_o\oint_{\mathrm{S}} n_j\varphi_i^*\mathrm{d}S \equiv -\rho_o\oint_{\mathrm{S}} n_i\varphi_j^*\mathrm{d}S. \qquad (2.20)$$

Thus, $\oint_{\mathrm{S}} Bn_i\mathrm{d}S \equiv \oint_{\mathrm{S}} B\mathbf{n}\cdot\nabla\varphi_i^*\mathrm{d}S$, and the divergence theorem therefore yields $\oint_{\mathrm{S}} Bn_i\mathrm{d}S = -\int_{\mathrm{V}}\mathrm{div}(\nabla\varphi_i^*B)\mathrm{d}^3\mathbf{y} \equiv -\int_{\mathrm{V}}\nabla\varphi_i^*\cdot\nabla B\mathrm{d}^3\mathbf{y}$. Substituting for ∇B from the momentum Equation (2.16), we obtain

$$\oint_{\mathrm{S}} Bn_i\mathrm{d}S = \int_V \mathrm{div}\left(\varphi_i^*\frac{\partial\mathbf{v}}{\partial t}\right)\mathrm{d}^3\mathbf{y} + \int_V\nabla\varphi_i^*\cdot\boldsymbol{\omega}\wedge\mathbf{v}\mathrm{d}^3\mathbf{y} - \nu\int_V\mathrm{div}(\nabla\varphi_i^*\wedge\boldsymbol{\omega})\mathrm{d}^3\mathbf{y}. \qquad (2.21)$$

The first and last integrals are further transformed by the divergence theorem:

$$\int_V\mathrm{div}\left(\varphi_i^*\frac{\partial\mathbf{v}}{\partial t}\right)\mathrm{d}^3\mathbf{y} = \frac{M_{ij}}{\rho_o}\frac{\mathrm{d}U_j}{\mathrm{d}t}, \qquad -\nu\int_V\mathrm{div}(\nabla\varphi_i^*\wedge\boldsymbol{\omega})\mathrm{d}^3\mathbf{y} = \nu\oint_{\mathrm{S}}\nabla\varphi_i^*\cdot\boldsymbol{\omega}\wedge\mathrm{d}\mathbf{S}.$$

Hence, substituting for $\oint_S Bn_i \mathrm{d}S$ in (2.19), we obtain

$$\left.\begin{aligned} \frac{\mathrm{d}G_i}{\mathrm{d}t} &= \Delta\frac{\mathrm{d}U_i}{\mathrm{d}t} + \frac{M_{ij}}{\rho_o}\frac{\mathrm{d}U_j}{\mathrm{d}t} - \int_V \nabla Y_i\cdot\boldsymbol{\omega}\wedge\mathbf{v}\mathrm{d}^3\mathbf{y} - \nu\oint_S \nabla Y_i\cdot\boldsymbol{\omega}\wedge\mathrm{d}\mathbf{S}, \\ &\text{where } Y_i = y_i - \varphi_i^*(\mathbf{y}). \end{aligned}\right\}, \tag{2.22}$$

The vector $\mathbf{Y}(\mathbf{y})$ (with its time dependence suppressed) will be called the *Kirchhoff vector* for the body. Like φ_i^*, it is determined by the shape of S; $Y_i(\mathbf{y})$ is just the velocity potential of incompressible flow past S having unit speed in the i-direction at large distances from S (with normal derivative $\partial Y_i/\partial y_n = 0$ on S).

Finally, the identity

$$\nabla Y_i\cdot\boldsymbol{\omega}\wedge\mathbf{U} = \mathrm{div}\Big(\mathbf{U}(\mathbf{v}\cdot\nabla Y_i) - \mathbf{v}(\mathbf{U}\cdot\nabla Y_i) - (\mathbf{v}\cdot\mathbf{U})\nabla Y_i\Big)$$

implies that $\int_V \nabla Y_i\cdot\boldsymbol{\omega}\wedge\mathbf{U}\,\mathrm{d}^3\mathbf{y} = 0$, and the use of this in (2.22) leads to the desired representation of $\mathrm{d}\mathbf{G}/\mathrm{d}t$ in terms of the vortex force $\boldsymbol{\omega}\wedge\mathbf{v}$:

$$\frac{\mathrm{d}G_i}{\mathrm{d}t} = \Delta\frac{\mathrm{d}U_i}{\mathrm{d}t} + \frac{M_{ij}}{\rho_o}\frac{\mathrm{d}U_j}{\mathrm{d}t} - \int_V \nabla Y_i\cdot\boldsymbol{\omega}\wedge\mathbf{v}_{\mathrm{rel}}d^3\mathbf{y} - \nu\oint_S \nabla Y_i\cdot\boldsymbol{\omega}\wedge\mathrm{d}\mathbf{S} \tag{2.23}$$

where $\mathbf{v}_{\mathrm{rel}} = \mathbf{v} - \mathbf{U}$ is the fluid velocity relative to the translational velocity of S.

The first two terms on the right of this equation depend only on the shape and volume of S, and on the acceleration $\mathrm{d}\mathbf{U}/\mathrm{d}t$: they determine the *irrotational* component of $\mathrm{d}\mathbf{G}/\mathrm{d}t$ produced by acceleration of the fluid displaced by S and its added mass. The influence of 'free field' vorticity is furnished by the volume integral. Because $\mathbf{v}_{\mathrm{rel}} = \mathbf{0}$ on S, the contribution to this integral from vorticity close to and on S is negligible; this is also true when the motion is regarded as inviscid, since then bound vorticity in the form of a vortex sheet occurs on S, where ∇Y_i and $\boldsymbol{\omega}\wedge\mathbf{v}_{\mathrm{rel}}$ are orthogonal vectors. The final (surface) integral in (2.23) gives the overall contribution from surface friction, which is relatively small when the Reynolds number is large.

It now follows from (2.13) that the force exerted on the fluid by S can be written

$$F_i = M_{ij}\frac{\mathrm{d}U_j}{\mathrm{d}t} - \rho_o\int_V \nabla Y_i\cdot\boldsymbol{\omega}\wedge\mathbf{v}_{\mathrm{rel}}\mathrm{d}^3\mathbf{y} - \eta\oint_S \nabla Y_i\cdot\boldsymbol{\omega}\wedge\mathrm{d}\mathbf{S}, \tag{2.24}$$

where $\eta = \rho_o\nu$ is the shear coefficient of viscosity. An alternative derivation of this formula is given in [24]. The first term on the right is the force necessary to accelerate the added mass, which generally depends on the direction of motion. The i-component of the usual viscous 'skin friction' is $-\eta\oint_S(\boldsymbol{\omega}\wedge\mathrm{d}\mathbf{S})_i \equiv -\eta\oint_S \nabla y_i\cdot\boldsymbol{\omega}\wedge\mathrm{d}\mathbf{S}$. Thus (because $Y_i = y_i - \varphi_i^*$) the net contribution of the normal pressure forces on S is represented in (2.24) by the terms

$$-\rho_o\int_V \nabla Y_i\cdot\boldsymbol{\omega}\wedge\mathbf{v}_{\mathrm{rel}}\mathrm{d}^3\mathbf{y} + \eta\oint_S \nabla\varphi_i^*\cdot\boldsymbol{\omega}\wedge\mathrm{d}\mathbf{S}.$$

The second, viscous component is comparable in magnitude to the skin friction, and is produced by the pressure field established by the surface shear stress.

The necessity for such a term is vividly illustrated by the Stokes drag on a sphere. Let the sphere have radius R and translate at constant velocity $\mathbf{U} = (-U, 0, 0),\ U > 0$, along the y_1-axis. At very small Reynolds numbers $\mathrm{Re} = 2RU/\nu \ll 1$ the vorticity $\boldsymbol{\omega} = \mathrm{curl}\,(3R\mathbf{U}/2|\mathbf{y}|)$ [18, Section 4.9], where the coordinate origin is taken at the centre of the sphere. When the

motion is slow enough for inertia forces to be ignored, the net drag (in the y_1-direction) is determined by the final term on the right of (2.24), being equal to $-F_1 = D_s + D_p$, where $D_s,\ D_p$ correspond respectively to the skin friction and viscous pressure contributions. For the sphere $\varphi_1^* = -R^3 y_1/2|\mathbf{y}|^3$, and we readily calculate that the net Stokes drag $-F_1 = 6\pi\eta U R$ has the components

$$D_s = \eta \oint_S (\boldsymbol{\omega} \wedge \mathrm{d}\mathbf{S})_1 = 4\pi\eta U R, \quad D_p = -\eta \oint_S \nabla\varphi_1^* \cdot \boldsymbol{\omega} \wedge \mathrm{d}\mathbf{S} = 2\pi\eta U R.$$

The pressure drag is therefore equal to half the skin-friction drag. This interpretation of the component forces is in accord with the 'creeping flow' approximation $\nabla p = -\eta \mathrm{curl}\,\boldsymbol{\omega}$ (which is used to derive the Stokes drag formula) and the following sequence of transformations

$$D_p = -\oint_S p n_1 \mathrm{d}S \equiv -\oint_S p \nabla\varphi_1^* \cdot \mathrm{d}\mathbf{S} = \int_V \nabla p \cdot \nabla\varphi_1^* \mathrm{d}^3\mathbf{y} = -\eta \int_V \mathrm{curl}\,\boldsymbol{\omega} \cdot \nabla\varphi_1^* \mathrm{d}^3\mathbf{y} =$$
$$-\eta \oint_S \nabla\varphi_1^* \cdot \boldsymbol{\omega} \wedge \mathrm{d}\mathbf{S}.$$

2.4. Deductions from the equation of vortex sound

The substitution of (2.23) in Equation (2.12) yields the following dipole acoustic field produced by compact flow-structure interaction for a non-rotating body:

$$p(\mathbf{x}, t) \approx \frac{x_i}{4\pi c_o |\mathbf{x}|^2} \frac{\partial}{\partial t} \left[(\rho_o \Delta\delta_{ij} + M_{ij}) \frac{\mathrm{d}U_j}{\mathrm{d}t} - \rho_o \int_V \nabla Y_i \cdot \boldsymbol{\omega} \wedge \mathbf{v}_{\mathrm{rel}} \mathrm{d}^3\mathbf{y} - \eta \oint_S \nabla Y_i \cdot \boldsymbol{\omega} \wedge \mathrm{d}\mathbf{S} \right], \quad |\mathbf{x}| \to \infty. \tag{2.25}$$

The three terms in the square braces respectively represent the dipole strengths produced by accelerated motion of S, the normal stress on S produced by the free-field vorticity, and surface friction forces. The latter can be discarded at very large Reynolds numbers, in which case the representation becomes independent of the bound vorticity.

Equation (2.25) can be derived also from the vortex sound Equation (1.8). The calculations are very straightforward when the motions of S are limited to small amplitude translational oscillations, and we shall confine attention to this case. The motion in the source region can be regarded as incompressible, so that when also nonlinear effects on the propagation of sound are ignored, and the mean flow is at rest at infinity, Equation (1.8) reduces to

$$\left(\frac{1}{c_o^2} \frac{\partial^2}{\partial t^2} - \nabla^2 \right) B = \mathrm{div}(\boldsymbol{\omega} \wedge \mathbf{v}). \tag{2.26}$$

This is solved by means of a Green's function $\mathcal{G}(\mathbf{x}, \mathbf{y}, t - \tau)$ that satisfies

$$\left(\frac{1}{c_o^2} \frac{\partial^2}{\partial \tau^2} - \frac{\partial^2}{\partial y_j^2} \right) \mathcal{G} = \delta(\mathbf{x} - \mathbf{y})\delta(t - \tau), \quad \mathcal{G} = 0 \text{ for } \quad \tau > t, \tag{2.27}$$

and has vanishing normal derivatives $\partial\mathcal{G}/\partial x_n,\ \partial\mathcal{G}/\partial y_n$ respectively for $\mathbf{x}$ and $\mathbf{y}$ on S. The application of Green's theorem in the usual way (see, *e.g.* [9, Section 1.10], [21, Section 7.6], [22, Section 12.2], [25, Section 5.1]) then supplies the solution of (2.26) in the form

$$B(\mathbf{x},t) = -\oint_S \mathcal{G}(\mathbf{x},\mathbf{y},t-\tau)\frac{\partial B}{\partial y_j}(\mathbf{y},\tau)\mathrm{d}S_j(\mathbf{y})\mathrm{d}\tau + \int \mathcal{G}(\mathbf{x},\mathbf{y},t-\tau)\frac{\partial}{\partial y_j}(\boldsymbol{\omega}\wedge\mathbf{v})_j(\mathbf{y},\tau)\mathrm{d}^3\mathbf{y}\mathrm{d}\tau. \tag{2.28}$$

The divergence theorem yields $\int \mathcal{G}\mathrm{div}(\boldsymbol{\omega}\wedge\mathbf{v})\mathrm{d}^3\mathbf{y} = -\oint_S \mathcal{G}(\boldsymbol{\omega}\wedge\mathbf{v})_j\mathrm{d}S_j - \int(\boldsymbol{\omega}\wedge\mathbf{v})\cdot\nabla\mathcal{G}\mathrm{d}^3\mathbf{y}$. Thus, when the negligibly small influence of *bulk* viscosity on S is neglected, the momentum equation can be taken in the form (2.16) so that $\nabla B + \boldsymbol{\omega}\wedge\mathbf{v} = -\partial\mathbf{v}/\partial t - \nu\,\mathrm{curl}\,\boldsymbol{\omega}$, and (2.28) can be written

$$B(\mathbf{x},t) \approx -\int(\boldsymbol{\omega}\wedge\mathbf{v})_j(\mathbf{y},\tau)\frac{\partial\mathcal{G}}{\partial y_j}(\mathbf{x},\mathbf{y},t-\tau)\mathrm{d}^3\mathbf{y}\mathrm{d}\tau + \nu\oint_S \boldsymbol{\omega}(\mathbf{y},\tau)\wedge\frac{\partial\mathcal{G}}{\partial\mathbf{y}}(\mathbf{x},\mathbf{y},t-\tau)\cdot\mathrm{d}\mathbf{S}(\mathbf{y})d\tau$$
$$+\oint_S \mathcal{G}(\mathbf{x},\mathbf{y},t-\tau)\frac{\partial v_j}{\partial\tau}(\mathbf{y},\tau)\mathrm{d}S_j(\mathbf{y})\mathrm{d}\tau. \tag{2.29}$$

This can be evaluated *correct to dipole order* by using the *compact* approximation for $\mathcal{G}$ [9]:

$$\mathcal{G}(\mathbf{x},\mathbf{y},t-\tau) = \frac{1}{4\pi\,|\mathbf{X}-\mathbf{Y}|}\delta\left(t-\tau-\frac{|\mathbf{X}-\mathbf{Y}|}{c_o}\right). \tag{2.30}$$

In this formula $\mathbf{Y} = (Y_1(\mathbf{y}), Y_2(\mathbf{y}), Y_3(\mathbf{y}))$ is the Kirchhoff vector for *stationary* S, defined as in (2.22) and $\mathbf{X}(\mathbf{x})$ is defined similarly in terms of $\mathbf{x}$. The right-hand side of (2.30) is an approximate solution of (2.27) that agrees with the exact Green's function when the latter is expanded in a multipole series and all terms of quadrupole order and higher are discarded, and when *either* $\mathbf{x}$ or $\mathbf{y}$ lies in the far field of the body. Thus, (2.30) may be used when it is known that S is acoustically compact for the particular application at hand (so that the characteristic acoustic wavelength λ is large compared to the dimensions of S; see Figure 3). When $\mathbf{x}$ lies in the acoustic far field, the expansion of $\mathcal{G}$ to dipole order in the retarded time element $\mathbf{x}\cdot\mathbf{Y}/c_o|\mathbf{x}|$ supplies

$$\mathcal{G}(\mathbf{x},\mathbf{y},t-\tau) \approx \frac{1}{4\pi|\mathbf{x}|}\left(\delta(t-\tau-|\mathbf{x}|/c_o) + \frac{x_jY_j}{c_o|\mathbf{x}|}\delta'(t-\tau-|\mathbf{x}|/c_o)\right), \quad |\mathbf{x}|\to\infty, \tag{2.31}$$

where the prime denotes differentiation with respect to t. The far-field solution (2.25) (where $B = p/\rho_o$) is now recovered by inserting (2.31) into the integrals of (2.29), observing that there is no contribution from the (*monopole*) component $\delta(t-\tau-|\mathbf{x}|/c_o)$ of (2.31), and invoking the definition (2.20) of the added mass.

3. Vortex sound sources adjacent to a large surface

3.1. The plane wall

Turn attention now to sound production by low-Mach-number vorticity adjacent to a non-compact surface. The simplest canonical configuration is illustrated in Figure 4a, which shows a turbulent eddy of length scale ℓ adjacent to a rigid wall. If the wall coincides with the plane $x_2 = 0$ with the fluid occupying the half-space $x_2 > 0$, we can take $\mathrm{H}(f) \equiv \mathrm{H}(x_2)$ in the Ffowcs Williams - Hawkings equation (2.5). At high Reynolds number, when surface shear stresses are discarded, the solution (2.7) at a point $\mathbf{x}$ *within the flow* becomes

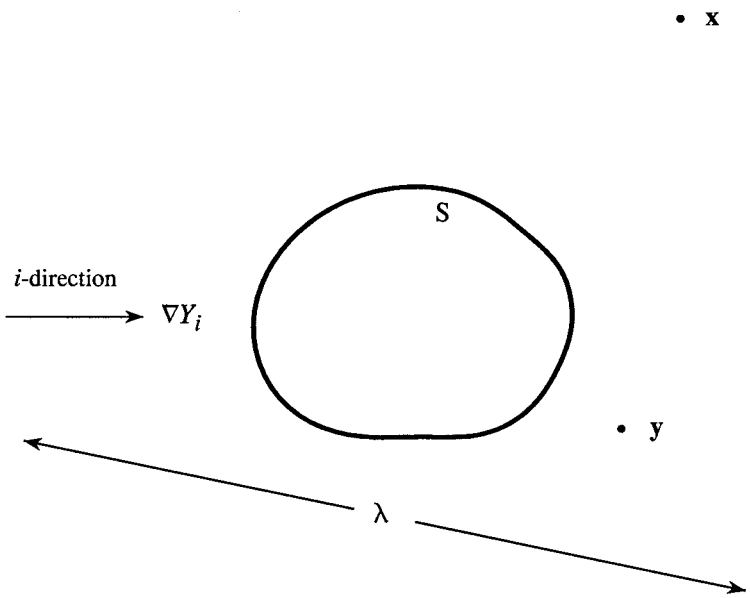

Figure 3. Illustrating the definition of the compact Green's function. One of either the source point **y** or observer position **x** must be in the far field of S, whose diameter must be much smaller than the characteristic wavelength of the sound. The component $Y_i(\mathbf{y})$ of the Kirchhoff vector represents the velocity potential of an incompressible flow at undisturbed unit speed in the i-direction that has vanishing normal velocity on S.

$$p(\mathbf{x},t)=\frac{\partial^2}{\partial x_i\partial x_j}\int_{y_2>0}\frac{(\rho_o v_i v_j)(\mathbf{y},t-|\mathbf{x}-\mathbf{y}|/c_o)}{4\pi|\mathbf{x}-\mathbf{y}|}\mathrm{d}^3\mathbf{y}-\frac{\partial}{\partial x_2}\oint_{y_2=0}\frac{p'_{22}(\mathbf{y},t-|\mathbf{x}-\mathbf{y}|/c_o)}{4\pi|\mathbf{x}-\mathbf{y}|}\,\mathrm{d}y_1\mathrm{d}y_3,$$
$$x_2>0, \qquad (3.1)$$

in which there is no contribution from the final 'monopole' term of (2.7) because $v_2=0$ on S.

The argument of Section 2.2 would suggest that the acoustic radiation is dominated by the dipole in (3.1), and that

$$p(\mathbf{x},t)\approx\frac{x_2}{4\pi|\mathbf{x}|^2c_o}\frac{\partial}{\partial t}\oint_{y_2=0}p'_{22}(\mathbf{y},t-|\mathbf{x}|/c_o)\mathrm{d}y_1\mathrm{d}y_3\sim\frac{\ell}{|\mathbf{x}|}\rho_o v^2M,\quad|\mathbf{x}|\to\infty.$$

But this is incorrect, because when retarded times are neglected the net normal force $\oint_{y_2=0}p'_{22}(\mathbf{y},t)\mathrm{d}y_1\mathrm{d}y_2$ between the fluid and wall vanishes. This is the Kraichnan-Phillips theorem [26–28]. Powell [29] pointed out that the surface dipoles actually represent the radiation produced by a system of quadrupoles formed by the *image* of the Reynolds stress distribution $\rho_o v_i v_j$. Indeed, application of (2.7) at the observer image point $(x_1,-x_2,x_3)$ (where $\mathrm{H}p\equiv0$), yields

$$0=\frac{\partial^2}{\partial x_i\partial x_j}\int_{y_2>0}\frac{(\rho_o v_i v_j)(\mathbf{y},t-|\mathbf{x}-\mathbf{y}'|/c_o)}{4\pi|\mathbf{x}-\mathbf{y}'|}\mathrm{d}^3\mathbf{y}+\frac{\partial}{\partial x_2}\oint_{y_2=0}\frac{p'_{22}(\mathbf{y},t-|\mathbf{x}-\mathbf{y}|/c_o)}{4\pi|\mathbf{x}-\mathbf{y}|}\mathrm{d}y_1\mathrm{d}y_3,$$
$$\mathbf{y}'=(y_1,-y_2,y_3). \qquad (3.2)$$

When this is combined with (3.1) the dipole terms disappear, and the net acoustic pressure is found to be determined by the direct radiation from the quadrupoles in $y_2>0$ augmented by that generated by their images in the wall (with a 'reflection coefficient' $\mathcal{R}=1$); the amplitude of the acoustic pressure $\sim(\ell/|\mathbf{x}|)\rho_o v^2M^2$, the same as for free space quadrupoles.

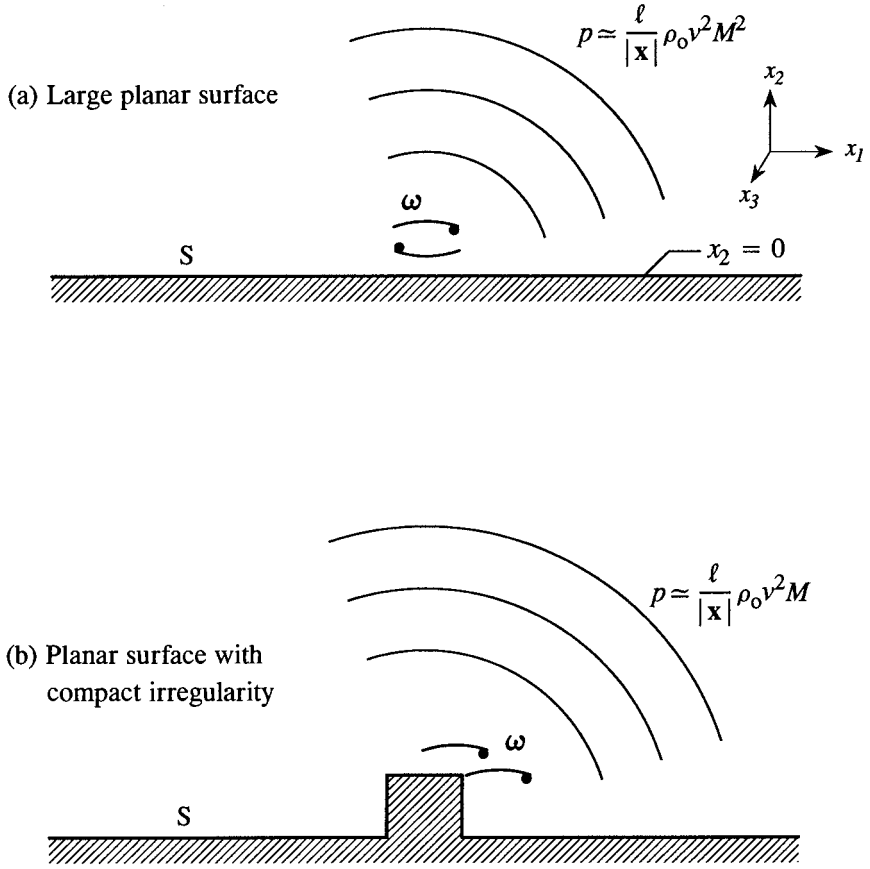

Figure 4. Sound generation by vorticity adjacent to a large planar surface (a) when the surface is perfectly flat, and (b) in the presence of a compact surface irregularity.

The same conclusion holds when contributions from surface *shear* stresses (which have been discarded from the dipole terms in (3.1) and (3.2), but correspond to 'dipole sources' with axes parallel to the wall) are included; the image system in this case is formed with $|\mathcal{R}| < 1$, and the amplitude and phase of $\mathcal{R}$ generally depend on frequency. Analogous results obtain for a homogeneous, flexible wall [30], but generally $\mathcal{R} \neq 1$ although $\mathcal{R} = O(1)$.

The situation is completely different for the case illustrated in Figure 4b, for turbulence in the vicinity of a small surface irregularity on a plane wall (or turbulence near a small body very close to the wall). In practice both the irregularity and the vorticity with which it interacts most strongly will have a similar length scale ℓ, say. We now deduce from (2.7) that the radiation at low Mach numbers can be attributed to the unsteady force on the irregularity parallel to the plane. The problem can be treated for rigid-surface conditions using the vortex sound Equation (2.26) and the corresponding compact Green's function

$$\left.\begin{aligned} \mathcal{G}(\mathbf{x},\mathbf{y},t-\tau) &= \tfrac{1}{4\pi|\mathbf{X}-\mathbf{Y}|}\delta\left(t-\tau-\tfrac{|\mathbf{X}-\mathbf{Y}|}{c_o}\right)+\tfrac{1}{4\pi|\mathbf{X}-\mathbf{Y}'|}\delta\left(t-\tau-\tfrac{|\mathbf{X}-\mathbf{Y}'|}{c_o}\right)\\ Y_i(\mathbf{y}) &= Y_i'(\mathbf{y}) = y_i-\varphi_i^*, \quad i=1,\ 3\\ Y_2(\mathbf{y}) &= -Y_2'(\mathbf{y}) = y_2 \end{aligned}\right\}, \tag{3.3}$$

which has vanishing normal derivative on the surface S of the wall and the irregularity. For $i = 1$ or 3, the component $Y_i(\mathbf{y})$ of the Kirchhoff vector is the velocity potential of ideal incompressible flow parallel to the wall normalized to have unit speed in the i-direction at large distances from the irregularity. ($Y_3 \equiv y_3$ in the particular case of a *two-dimensional* irregularity, uniform in the x_3-direction of Figure 4b.)

The general solution is given by Equation (2.29). The normal component of velocity vanishes on S, and in the acoustic far field $B(\mathbf{x}, t) = p(\mathbf{x}, t)/\rho_o$, where (3.3) becomes

$$\mathcal{G}(\mathbf{x}, \mathbf{y}, t-\tau) \approx \frac{1}{4\pi|\mathbf{x}|}\left\{2\delta(t-\tau-|\mathbf{x}|/c_o) + \frac{x_j(Y_j + Y_j')}{c_o|\mathbf{x}|}\delta'(t-\tau-|\mathbf{x}|/c_o)\right\}, \quad |\mathbf{x}| \to \infty. \tag{3.4}$$

Hence

$$\begin{aligned} p(\mathbf{x}, t) &\approx \frac{-x_\alpha}{2\pi c_o|\mathbf{x}|^2}\frac{\partial}{\partial t}\left[\rho_o\int_{\mathrm{V}}\nabla Y_\alpha\cdot\boldsymbol{\omega}\wedge\mathbf{v}\mathrm{d}^3\mathbf{y} + \eta\oint_{\mathrm{S}}\nabla Y_\alpha\cdot\boldsymbol{\omega}\wedge\mathrm{d}\mathbf{S}\right], \\ &= \frac{x_\alpha}{2\pi c_o|\mathbf{x}|^2}\frac{\partial}{\partial t}F_\alpha\left(t-\frac{|\mathbf{x}|}{c_o}\right) \sim \frac{\ell}{|\mathbf{x}|}\rho_o v^2 M, \quad |\mathbf{x}| \to \infty, \end{aligned} \tag{3.5}$$

where the repeated Greek subscript α is to be summed only over the 1- and 3-directions parallel to the wall, and F_α is the unsteady *drag* on the wall and irregularity.

3.2. The non-compact edge

An important practical problem concerns the production of sound by turbulence in the vicinity of the edge of a large surface S, which we shall take to be rigid, as illustrated schematically in Figure 5a. The Ffowcs Williams - Hawkings equation can again be used to express the radiation in a form similar to (3.1), consisting of the direct contribution from the turbulence quadrupole plus a contribution from a surface integral over S from normally orientated dipole sources. At low Mach numbers we may anticipate that the dipole radiation will be overwhelming large, and omit that from the quadrupoles [31], so that (2.7) reduces to

$$p(\mathbf{x}, t) = -\frac{\partial}{\partial x_i}\oint_{\mathrm{S}}\frac{[p_{ij}']}{4\pi|\mathbf{x}-\mathbf{y}|}\mathrm{dS}_j(\mathbf{y}). \tag{3.6}$$

The discussion of the infinite plane wall in Section 3.1 suggests that care should be exercised in evaluating this integral when the surface S extends into the acoustic far field of the edge sources. To examine this consider the simpler geometry of Figure 5b, where the turbulence is near the edge of a rigid *half-plane* $x_1 < 0,\ x_2 = 0$, and also set

$$p(\mathbf{x}, t) = \int_{-\infty}^{\infty} p(\mathbf{x}, \omega)\mathrm{e}^{-\mathrm{i}\omega t}\mathrm{d}\omega. \tag{3.7}$$

If the viscous contribution to the dipole strength is temporarily ignored, Equation (3.6) becomes, for each frequency ω,

$$\begin{aligned} p(\mathbf{x}, \omega) &\approx -\frac{\partial}{\partial x_2}\int_{-\infty}^{\infty}\mathrm{d}y_3\int_{-\infty}^{0}\Big(p_+ - p_-\Big)(\mathbf{y}, \omega)\frac{\mathrm{e}^{\mathrm{i}\kappa_o|\mathbf{x}-\mathbf{y}|}}{4\pi|\mathbf{x}-\mathbf{y}|}\,\mathrm{d}y_1 \\ &\sim \frac{-\mathrm{i}\kappa_o\sin\psi\sin\theta\mathrm{e}^{\mathrm{i}\kappa_o|\mathbf{x}|}}{4\pi|\mathbf{x}|}\int_{-\infty}^{\infty}\mathrm{d}y_3\int_{-\infty}^{0}\Big(p_+ - p_-\Big)(\mathbf{y}, \omega)\mathrm{e}^{-\mathrm{i}\kappa_o\mathbf{x}\cdot\mathbf{y}/|\mathbf{x}|}\,\mathrm{d}y_1, \\ &\qquad\qquad |\mathbf{x}| \to \infty, \end{aligned} \tag{3.8}$$

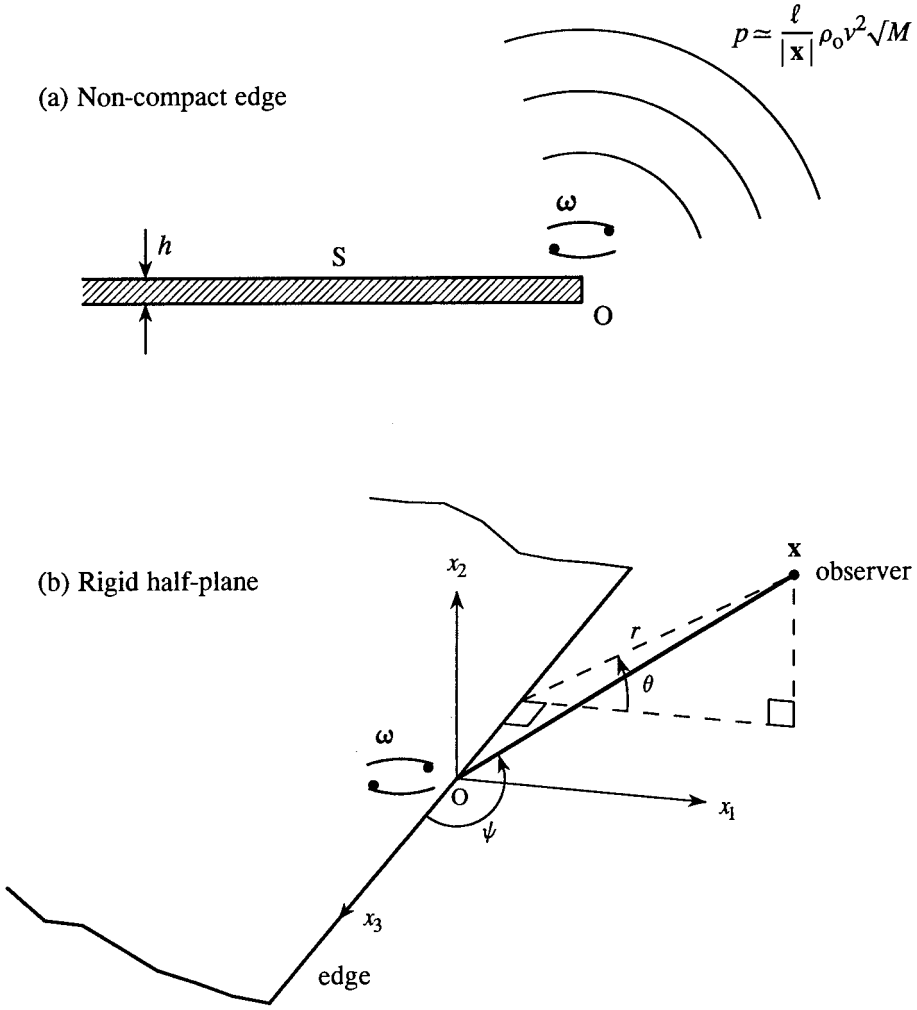

Figure 5. Sound generation by vorticity adjacent to (a) a noncompact edge of finite, but compact thickness h, (b) a rigid half-plane.

where $p_\pm \equiv p(y_1, \pm 0, y_3, \omega)$ denotes the pressure on the 'upper' and 'lower' faces of the half-plane, $\kappa_o = \omega/c_o$ is the acoustic wavenumber, and the angles ψ, θ define the orientation of the far field point **x**, as indicated in Figure 5b (ψ being the angle between the edge of the half-plane and the vector **x**).

Now set

$$p_\pm = p_\pm^{\mathrm{I}} + p_\pm^{\mathrm{A}}, \tag{3.9}$$

where $p_\pm^{\mathrm{I}}$, $p_\pm^{\mathrm{A}}$ denote respectively the hydrodynamic and acoustic contributions to the surface pressures, *i.e.* $p_\pm^{\mathrm{I}}$ is the surface pressure when the motion is regarded as incompressible. At low Mach numbers we might reasonably hope to estimate the acoustic pressure $p(\mathbf{x}, \omega)$ from (3.8) by setting $p_+ - p_- = p_+^{\mathrm{I}} - p_-^{\mathrm{I}}$, since the local motion near the edge, close to the turbulence is surely dominated by the incompressible pressure field.

To test this hypothesis suppose the turbulence is confined to the region $x_2 > 0$ above the half-plane and introduce the *blocked pressure* $p_s(x_1, x_3, t)$, which is defined to be the pressure

that the same turbulence would exert on an *infinite* plane wall at $x_2 = 0$. Then an exact calculation [32] shows that

$$p_+(\mathbf{x},\omega) - p_-(\mathbf{x},\omega) = -\frac{1}{2\pi i}\int_{-\infty}^{\infty} \frac{p_s(k_1,k_3,\omega)\sqrt{(\kappa_o^2-k_3^2)^{1/2}+k_1}}{\sqrt{(\kappa_o^2-k_3^2)^{1/2}+K_1}(K_1-k_1+i0)} \mathrm{e}^{\mathrm{i}\{K_1x_1+k_3x_3\}}\mathrm{d}K_1\mathrm{d}k_1\mathrm{d}k_3, \tag{3.10}$$

where $p_s(k_1,k_3,\omega) = \frac{1}{(2\pi)^2}\int_{-\infty}^{\infty} p_s(x_1,x_3,\omega)\mathrm{e}^{-\mathrm{i}(k_1x_1+k_3x_3)}\mathrm{d}x_1\mathrm{d}x_3$ is the spatial Fourier transform of the blocked pressure, and

$$(\kappa_o^2-k_3^2)^{1/2} = \begin{cases} \mathrm{sgn}(\omega)|\kappa_o^2-k_3^2|^{1/2} & \text{for } \kappa_o^2 > k_3^2, \\ +\mathrm{i}|\kappa_o^2-k_3^2|^{1/2} & \text{for } \kappa_o^2 < k_3^2. \end{cases}$$

The approximation $p_+ - p_- \approx p_+^{\mathrm{I}} - p_-^{\mathrm{I}}$ is given by the limiting value of (3.10) as $\kappa_o \to 0$. Using this in (3.8), and noting also that $p_+ - p_- \equiv 0$ when $y_1 > 0$, we find

$$\begin{aligned} p(\mathbf{x},\omega) &\approx \frac{\sqrt{\kappa_0}\sin\psi\sin\theta\mathrm{e}^{\mathrm{i}\kappa_0|\mathbf{x}|}}{2|\mathbf{x}|}\int_{-\infty}^{\infty} \frac{p_s\left(k_1,\dfrac{x_3\kappa_o}{|\mathbf{x}|},\omega\right)\sqrt{\mathrm{i}\dfrac{|x_3\kappa_o|}{|\mathbf{x}|}+k_1}}{\sqrt{\mathrm{i}\dfrac{|x_3|}{|\mathbf{x}|}+\dfrac{\mathrm{sgn}(\omega)x_1}{|\mathbf{x}|}}\left(\dfrac{\kappa_o x_1}{|\mathbf{x}|}-k_1+\mathrm{i}0\right)}dk_1 \\ &\sim \frac{-\sqrt{\kappa_0}\sin\psi\sin\theta\mathrm{e}^{\mathrm{i}\kappa_0|\mathbf{x}|}}{2|\mathbf{x}|\sqrt{\mathrm{i}\dfrac{|x_3|}{|\mathbf{x}|}+\dfrac{\mathrm{sgn}(\omega)x_1}{|\mathbf{x}|}}}\int_{-\infty}^{\infty}\frac{p_s(k_1,0,\omega)}{\sqrt{k_1+\mathrm{i}0}}\mathrm{d}k_1, \end{aligned} \tag{3.11}$$

where in the second line we have made the approximation $k_1 \gg \kappa_0$ in the integral, because at low Mach numbers $k_1 \sim 1/\ell$, where the hydrodynamic length scale $\ell \ll 1/\kappa_o \sim$ acoustic wavelength.

This result shows that the integral in (3.8) $\sim O(1/\sqrt{\kappa_o})$, and would therefore *diverge* if $p_+ - p_-$ were to be approximated by the incompressible pressure jump $p_+^{\mathrm{I}} - p_-^{\mathrm{I}}$ *and* the retarded time phase factor $\mathrm{e}^{-\mathrm{i}\kappa_o\mathbf{x}\cdot\mathbf{y}/|\mathbf{x}|}$ were replaced by unity. A numerical scheme that ignored this divergence would predict sound of amplitude $\sim (\ell/|\mathbf{x}|)\rho_o v^2 M$ radiated from the vicinity of the edge; the sound would consist of 'numerical noise' produced by a spurious edge-dipole orientated in the normal (x_2-) direction.

The integral in (3.11) is dominated by the hydrodynamic components of $p_s(k_1,0,\omega)$, where $k_1 \sim 1/\ell$. The order of magnitude of the acoustic pressure and its directivity are therefore found to be

$$p(\mathbf{x},t) \sim \frac{\sin\psi\sin\theta}{(\cos^2\psi+\sin^2\psi\cos^2\theta)^{\frac{1}{4}}}\left(\frac{\ell}{|\mathbf{x}|}\right)\rho_o v^2\sqrt{M}, \tag{3.12}$$

which for small Mach number M is larger by a factor $\sim 1/\sqrt{M}$ than the dipole radiation from turbulence close to a compact body, a result first predicted by Ffowcs Williams and Hall [31].

But the prediction (3.12) is unbounded for radiation directions normal to the surface ($\theta = \pm 90°,\ \psi = 90°$) (Figure 5b). This is because in deriving (3.11) full account has been taken of the geometry of the half-plane in calculating the hydrodynamic pressure fluctuations, but not in calculating the sound. The surface extends into the acoustic far field, and the surface integrals in (3.6) and (3.8) must actually include contributions that explicitly *represent the reflection of waves from the half-plane*; *i.e.* the pressure jump in (3.8) must include information about the *acoustic field* on S. When the exact pressure jump (3.10) across the half-plane is used in (3.8), the correct approximation to the far field sound becomes

$$p(\mathbf{x},\omega) \approx \frac{-\sqrt{\kappa_o}\sin^{\frac{1}{2}}\psi\sin(\theta/2)\mathrm{e}^{\mathrm{i}\kappa_o|\mathbf{x}|}}{\sqrt{2}|\mathbf{x}|}\int_{-\infty}^{\infty}\frac{p_s(k_1,0,\omega)}{\sqrt{k_1+\mathrm{i}0}}\mathrm{d}k_1$$
$$p(\mathbf{x},t) \sim \sin^{\frac{1}{2}}\psi\sin(\theta/2)\left(\frac{\ell}{|\mathbf{x}|}\right)\rho_o v^2\sqrt{M}. \tag{3.13}$$

This is bounded in all radiation directions, and in particular takes its largest values at $\theta = \pm 180^\circ$.

For a more general edge geometry (for example, Figure 5a), it may therefore be concluded that to calculate the dominant radiation at low Mach numbers from the Ffowcs Williams - Hawkings approximation (3.6), an estimate of the source strength based on incompressible flow theory will yield *at best* the correct order of magnitude of the sound pressure, but will not supply the correct directivity. This confirms that the edge is the dominant source of the sound, and that the effective source strength is determined by incompressible motions at the edge. We should therefore expect both the amplitude and the directivity of the radiation to be correctly predicted in terms of an incompressible model of the source strength provided Lighthill's equation is solved using a Green's function tailored to the surface geometry instead of the free space Green's function used in the Ffowcs Williams - Hawkings formula (2.7).

To do this let $p_q(\mathbf{x},\omega)$ denote the component of frequency ω of the pressure field generated by the volume quadrupoles when the presence of the surface S is ignored, i.e. let p_q be the *free space* solution of

$$(\nabla^2+\kappa_o^2)p_q = -\rho_o\frac{\partial^2 v_i v_j}{\partial x_i\partial x_j}. \tag{3.14}$$

Then $\bar{p}(\mathbf{x},\omega) = p - p_q$ satisfies

$$(\nabla^2+\kappa_o^2)\bar{p} = 0, \quad \nabla\bar{p}+\nabla p_q = -\eta\,\mathrm{curl}\,\boldsymbol{\omega} \quad \text{on S}. \tag{3.15}$$

Introduce a Green's function $\mathcal{G}(\mathbf{x},\mathbf{y},\omega)$ with outgoing wave behaviour that satisfies $(\nabla^2 + \kappa_o^2)\mathcal{G} = \delta(\mathbf{x}-\mathbf{y})$ and $\partial\mathcal{G}/\partial x_n = 0$, $\partial\mathcal{G}/\partial y_n = 0$ respectively for $\mathbf{x}$ and $\mathbf{y}$ on S. Then $\bar{p} = \oint_{\mathrm{S}}\mathcal{G}\,\partial\bar{p}/\partial y_n\,\mathrm{dS}$, and therefore

$$p(\mathbf{x},\omega) = p_q(\mathbf{x},\omega) - \oint_{\mathrm{S}}\mathcal{G}(\mathbf{x},\mathbf{y},\omega)\left(\frac{\partial p_q}{\partial\mathbf{y}}+\eta\,\mathrm{curl}\,\boldsymbol{\omega}\right)(\mathbf{y},\omega)\cdot\mathrm{d}\mathbf{S}. \tag{3.16}$$

In the integral p_q is the 'quadrupole' pressure field incident on S, produced by the neighbouring turbulent eddies. Those eddies lying in the far field of the edge produce sound waves that are merely diffracted at the edge, without changing the overall power of the radiated sound. However, those eddies whose near fields encompass the edge are responsible for a large increase in sound production, because of the scattering by the edge of the energetic hydrodynamic near field pressures. This contribution can be evaluated by expanding $\mathcal{G}(\mathbf{x},\mathbf{y},\omega)$ in terms of the nondimensional source distance $\kappa_o\sqrt{y_1^2+y_2^2}$ ($\sim\sqrt{y_1^2+y_2^2}$/acoustic wavelength) from the edge. When the observation point $\mathbf{x}$ recedes to the acoustic far field we find [9, Section 3.2]

$$\mathcal{G}(\mathbf{x},\mathbf{y},\omega) = \mathcal{G}_0(\mathbf{x},\mathbf{y},\omega)+\mathcal{G}_1(\mathbf{x},\mathbf{y},\omega)+\ldots, \tag{3.17}$$

where (when $|\mathbf{x}-y_3\mathbf{i}_3|\to\infty$ and $\kappa_o\sqrt{y_1^2+y_2^2}\ll 1$)

$$\mathcal{G}_0(\mathbf{x},\mathbf{y},\omega)=\frac{-1}{4\pi|\mathbf{x}-y_3\mathbf{i}_3|}\mathrm{e}^{\mathrm{i}\kappa_o|\mathbf{x}-y_3\mathbf{i}_3|},\quad \mathcal{G}_1(\mathbf{x},\mathbf{y},\omega)=\frac{-1}{\pi\sqrt{2\pi\mathrm{i}}}\frac{\sqrt{\kappa_o}\varphi^*(\mathbf{x})\Phi^*(\mathbf{y})}{|\mathbf{x}-y_3\mathbf{i}_3|^{3/2}}\mathrm{e}^{\mathrm{i}\kappa_o|\mathbf{x}-y_3\mathbf{i}_3|}. \tag{3.18}$$

In these formulae $\mathbf{i}_3$ is a unit vector parallel to the x_3-axis (the edge direction); the function $\Phi^*(\mathbf{y})\equiv\Phi^*(y_1,y_2)$ is equivalent to the velocity potential of a two-dimensional, incompressible flow around the edge in the anticlockwise sense in Figure 5a, normalized such that (when the argument $\mathbf{y}$ is replaced by $\mathbf{x}$)

$$\Phi^*(\mathbf{x})\to\varphi^*(\mathbf{x})\equiv\sqrt{r}\sin(\theta/2)\equiv\sqrt{|\mathbf{x}|}\sin^{\frac{1}{2}}\psi\sin(\theta/2)\ \text{ for }\ \sqrt{x_1^2+x_2^2}\gg h, \tag{3.19}$$

where h is the thickness of the edge, and (r,θ) are the polar coordinates $(x_1,x_2)=r(\cos\theta,\sin\theta)$ defined as in Figure 5b. The function $\varphi^*(\mathbf{x})$ is the velocity potential of flow around an edge of zero thickness, *i.e.* around the half-plane of Figure 5b. The component $\mathcal{G}_0$ represents the radiation from a point source at $\mathbf{y}$ when scattering by the surface is neglected. The component $\mathcal{G}_1$ provides the first correction due to the presence of S, and (since $\mathcal{G}_0$ is independent of $y_1,\ y_2$) gives the leading approximation to the edge noise when used in (3.16).

For the *half-plane* problem of Figure 5b, the substitution of (3.17) in (3.16) yields

$$p(\mathbf{x},\omega)\approx p_q(\mathbf{x},\omega)-\int_{-\infty}^{\infty}\mathrm{d}y_3\int_{-\infty}^{0}\frac{\partial p_q}{\partial y_2}(y_1,0,y_3,\omega)\Big[\mathcal{G}_1(\mathbf{x},\mathbf{y},\omega)\Big]_-^+\mathrm{d}y_1 \tag{3.20}$$

at high Reynolds number, where $[\mathcal{G}_1]_-^+=\mathcal{G}_1(\mathbf{x},y_1,+0,y_3,\omega)-\mathcal{G}_1(\mathbf{x},y_1,-0,y_3,\omega)$. Consider the particular the case in which the turbulence is confined to $x_2>0$ 'above' the half-plane. The quadrupole pressure determined by (3.14) impinging on S can be expressed in terms of the blocked pressure p_s, defined as on the right of (3.10). Then the *hydrodynamic* component of $\partial p_q(y_1,0,y_3,,\omega)/\partial y_2=\frac{1}{2}\int_{-\infty}^{\infty}|k|p_s(k_1,k_3,\omega)\mathrm{e}^{\mathrm{i}(k_1y_1+k_3y_3)}\mathrm{d}k_1\mathrm{d}k_3$, and therefore (3.18) (with $\Phi^*(\mathbf{y})\equiv\varphi^*(\mathbf{y})$ for the half-plane) supplies

$$p(\mathbf{x},\omega)\approx p_q(\mathbf{x},\omega)-\frac{\mathrm{i}\sqrt{2\mathrm{i}\kappa_o}\sin^{\frac{1}{2}}\psi\sin(\theta/2)\mathrm{e}^{\mathrm{i}\kappa_o|\mathbf{x}|}}{\sqrt{\pi}|\mathbf{x}|}\times\int_{-\infty}^{\infty}|k_1|p_s(k_1,0,\omega)\left(\int_{-\infty}^{0}|y_1|^{\frac{1}{2}}\mathrm{e}^{\mathrm{i}k_1y_1}\mathrm{d}y_1\right)\mathrm{d}k_1,\quad |\mathbf{x}|\to\infty, \tag{3.21}$$

where we have made the additional approximation $p_s(k_1,\kappa_o\cos\psi,\omega)=p_s(k_1,0,\omega)$, which is applicable in the hydrodynamic domain. The y_1-integral in this result must be interpreted as the Fourier transform of a generalized function [33], with value $(-1/2|k_1|)\sqrt{\pi\mathrm{i}/(k_1+i0)}$. The second term on the right of (3.21) is then identical with the first line of the 'exact' representation (3.13) derived from the dipole term of the Ffowcs Williams - Hawkings equation.

3.3. Vortex sound theory for a non-compact edge

A direct representation of the edge noise in terms of the vorticity, without having recourse to the intermediary of the free space surface pressure gradient $\partial p_q/\partial y_n$, can be obtained from the general solution (2.29) of the vortex sound equation (2.26). For a stationary edge, located well within the hydrodynamic near field of the sources, the expansion (3.17) of Green's function yields

$$p(\mathbf{x},\omega) \approx \frac{-\rho_0\sqrt{\kappa_o}\sin^{\frac{1}{2}}\psi\sin(\theta/2)\mathrm{e}^{\mathrm{i}\kappa_o|\mathbf{x}|}}{\pi\sqrt{2\pi\mathrm{i}}|\mathbf{x}|}\left\{\int_{\mathrm{V}}\frac{\partial\Phi^*(\mathbf{y})}{\partial\mathbf{y}}\cdot\Big(\boldsymbol{\omega}\wedge\mathbf{v}\Big)(\mathbf{y},\omega)\mathrm{d}^3\mathbf{y}\right.$$
$$\left.-\,\nu\oint_{\mathrm{S}}\boldsymbol{\omega}(\mathbf{y},\omega)\wedge\frac{\partial\Phi^*(\mathbf{y})}{\partial\mathbf{y}}\cdot\mathrm{d}\mathbf{S}(\mathbf{y})\right\},\quad |\mathbf{x}|\to\infty. \tag{3.22}$$

The radiated sound automatically satisfies the rigid-surface boundary condition on the distant parts of S lying in the acoustic far field, so that the vorticity $\boldsymbol{\omega}$ and the velocity $\mathbf{v}$ in the integrands can be approximated by their values for incompressible flow near the edge.

For a stationary compact body the radiation is dominated by a dipole whose strength is just equal to the net force between the solid and fluid. A similar conclusion can be drawn from (3.22): the term in the brace brackets of (3.22) is proportional to the component of frequency ω of the unsteady force $F(t) = \int_{-\infty}^{\infty}F(\omega)\mathrm{e}^{-\mathrm{i}\omega t}\mathrm{d}\omega$ exerted on the fluid in the x_2-direction. This force increases in proportion to the square root of the acoustic wavelength, and is given by [34]

$$F(\omega)\approx 2\rho_0\sqrt{\frac{\mathrm{i}}{\pi\kappa_0}}\left\{\int_{\mathrm{V}}\frac{\partial\Phi^*(\mathbf{y})}{\partial\mathbf{y}}\cdot\Big(\boldsymbol{\omega}\wedge\mathbf{v}\Big)(\mathbf{y},\omega)\mathrm{d}^3\mathbf{y}-\ \nu\oint_{\mathrm{S}}\boldsymbol{\omega}(\mathbf{y},\omega)\wedge\frac{\partial\Phi^*(\mathbf{y})}{\partial\mathbf{y}}\cdot\mathrm{d}\mathbf{S}(\mathbf{y})\right\}.$$

An alternative form of the solution (3.22) is sometimes useful, especially in applications to boundary-layer-generated noise in mean flow over the edge. This is derived by first defining $B_q(\mathbf{x},t)$ to be the *free space* solution of (2.26), when the presence of S is temporarily ignored (*cf.* the definition of p_q in Section 3.2). Then set

$$B(\mathbf{x},t) = \bar{B}(\mathbf{x},t) + B_q(\mathbf{x},t), \tag{3.23}$$

where $\bar{B}$ satisfies the homogeneous form of (2.26), where the right-hand side is replaced by zero. $\bar{B}$ and B_q are related by the no-slip boundary condition on S:

$$\nabla\bar{B} + \nabla B_q = -\nu\mathrm{curl}\,\boldsymbol{\omega}\quad\text{on S}. \tag{3.24}$$

Proceeding as in the treatment of Equations (3.14), (3.15) we find for each frequency ω

$$p(\mathbf{x},\omega)\approx\frac{\rho_o\sqrt{\kappa_o}\sin^{\frac{1}{2}}\psi\sin(\theta/2)\mathrm{e}^{\mathrm{i}\kappa_0|\mathbf{x}|}}{\pi\sqrt{2\pi\mathrm{i}}|\mathbf{x}|}\oint_{\mathrm{S}}\left(\Phi^*(\mathbf{y})\frac{\partial B_q}{\partial\mathbf{y}}(\mathbf{y},\omega)+\nu\boldsymbol{\omega}(\mathbf{y},\omega)\wedge\frac{\partial\Phi^*(\mathbf{y})}{\partial\mathbf{y}}\right)\cdot\mathrm{d}\mathbf{S}(\mathbf{y}),$$
$$|\mathbf{x}|\to\infty, \tag{3.25}$$

where the integrand is to be evaluated using incompressible approximations for $\partial B_q/\partial\mathbf{y}$ and $\boldsymbol{\omega}$, and the quadrupole term $B_q \approx p_q/\rho_o$ has been neglected in the acoustic far field.

This result can be expressed in terms of the incompressible 'upwash' velocity $\mathbf{v}_q(\mathbf{x},t)$ defined by

$$\frac{\partial\mathbf{v}_q}{\partial t} = -\nabla B_q - \boldsymbol{\omega}\wedge\mathbf{v} = -\mathrm{curl}\int_{\mathrm{V}}\frac{\mathrm{curl}\,(\boldsymbol{\omega}\wedge\mathbf{v})\mathrm{d}^3\mathbf{y}}{4\pi|\mathbf{x}-\mathbf{y}|}. \tag{3.26}$$

The integrand in this formula decays rapidly to zero within the viscous sublayer on S, so that the integration can be confined to the region V_δ, say, where viscous effects are unimportant. In V_δ the transport of vorticity by viscous diffusion can be ignored, and the right-hand side of the vorticity equation $\partial\boldsymbol{\omega}/\partial t + \mathrm{curl}\,(\boldsymbol{\omega}\wedge\mathbf{v}) = \nu\nabla^2\boldsymbol{\omega}$ may be discarded. The upwash velocity can therefore be taken in the form

$$\mathbf{v}_q(\mathbf{x},t) = \operatorname{curl}\int_{V_\delta} \frac{\boldsymbol{\omega}(\mathbf{y},t)\mathrm{d}^3\mathbf{y}}{4\pi|\mathbf{x}-\mathbf{y}|}, \tag{3.27}$$

which is the Biot-Savart formula (1.3) with the integration confined to the region outside the viscous controlled sublayer on S. On S: $\partial\mathbf{v}_q/\partial t = -\nabla B_q$, so that (3.25) becomes

$$p(\mathbf{x},\omega) \approx \frac{\rho_o\sqrt{\kappa_o}\sin^{\frac{1}{2}}\psi\sin(\theta/2)\mathrm{e}^{\mathrm{i}\kappa_o|\mathbf{x}|}}{\pi\sqrt{2\pi\mathrm{i}}|\mathbf{x}|}\oint_S\left(\mathrm{i}\omega\Phi^*(\mathbf{y})\mathbf{v}_q(\mathbf{y},\omega)+\nu\boldsymbol{\omega}(\mathbf{y},\omega)\wedge\frac{\partial\Phi^*(\mathbf{y})}{\partial\mathbf{y}}\right)\cdot\mathrm{d}\mathbf{S}(\mathbf{y}),$$
$$|\mathbf{x}|\to\infty. \tag{3.28}$$

4. Vortex methods in action

The application of vortex methods to flow-structure interactions will now be illustrated by brief discussions of the generation of lift by an impulsively started airfoil, of the acoustic properties of the 'vortex whistle' [35–37], and of low-frequency pressure transients produced when a high-speed train enters a tunnel.

4.1. Lift developed by a two-dimensional airfoil

A two-dimensional airfoil of chord $2a$ and small angle of attack α is impulsively set into motion at time $t = 0$ at speed U in the negative x_1-direction (Figure 6a). Take the x_2-axis in the direction of mean lift, with the coordinate origin at the midchord position, translating with the airfoil. To first order in α it may be assumed that vorticity shed from the trailing edge in accordance with the *Kutta* condition [18, Section 6.7], [21, Section 3.8] occupies a vortex sheet on the x_1-axis between $x_1 = a$ and $x_1 = a + Ut$.

For an incompressible fluid the circulation $\mathcal{K}(x_1,t)$ per unit length of the wake is given by [38], [39, Section 6.7]

$$\mathcal{K}(x_1,t) = \frac{2\alpha U}{\pi}\int_{-\infty}^{\infty}\frac{\mathrm{e}^{-\mathrm{i}k(Ut-x_1)}\mathrm{d}k}{(k+\mathrm{i}0)[\mathrm{H}_0^{(1)}(ka)+\mathrm{i}\mathrm{H}_1^{(1)}(ka)]}, \quad a<x_1<a+Ut. \tag{4.1}$$

This integral is readily evaluated numerically and provides sufficient information to calculate the unsteady lift from (2.24). The classical procedure based on the impulse formula (2.13) requires *in addition* a knowledge of the *bound vorticity* on the airfoil.

The circulation in the wake at time t is $\int_a^{a+Ut}\mathcal{K}(x_1,t)\mathrm{d}x_1$, and tends to $\Gamma \equiv 2\pi\alpha aU$ as $Ut/a \to \infty$; it is plotted as the broken line curve in Figure 6b. All of the vorticity is effectively shed from the airfoil when Ut/a exceeds about 10. The upper part of Figure 6b shows successive positions of the centroid of the wake vorticity: $x_c(t) = a + \int_a^{a+Ut}(x_1 - a)\mathcal{K}(x_1,t)\mathrm{d}x_1 / \int_a^{a+Ut}\mathcal{K}(x_1,t)\mathrm{d}x_1$. The free vorticity occupies the vortex sheet $\boldsymbol{\omega} = \mathbf{i}_3\mathcal{K}(x_1,t)\,\delta(x_2)$ $(a < x_1 < a + Ut)$, where $\mathbf{i}_3$ is a unit vector in the spanwise (x_3-) direction, out of the plane of the paper in Figure 6a, and to first order in α it convects at constant speed U relative to the airfoil in the x_1-direction. When viscous forces are ignored, the lift *per unit span* of the airfoil is therefore predicted by (2.24) to be

$$\text{Lift} = -F_2 = \rho_o U\int_a^{a+Ut}\mathcal{K}(x_1,t)\left(\frac{\partial X_2}{\partial x_2}\right)_{x_2=0}\mathrm{d}x_1, \tag{4.2}$$

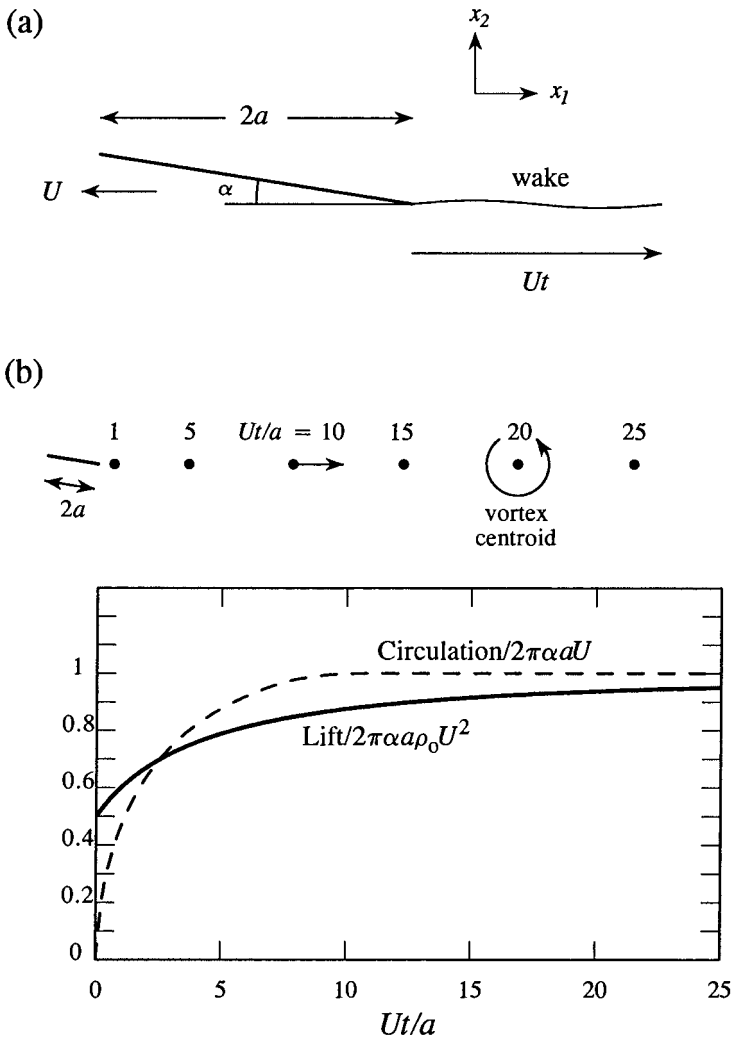

Figure 6. (a) A thin plate airfoil moves to the left at constant speed U, starting impulsively from rest at time $t = 0$. (b) Growth of the lift and circulation as a function of time, and the locations of the centroid of the wake at different times.

where $X_2(x_1, x_2)$ is the x_2-component of the Kirchhoff vector (the velocity potential of flow past the airfoil having unit speed in the x_2-direction at large distances from the airfoil). When $Ut/a \gg 1$ the shed vorticity is far downstream of the airfoil, where $\partial X_2/\partial x_2 \to 1$, and the asymptotic lift tends to the *Kutta-Joukowski* value: $\rho_o U \int_a^{a+Ut} \mathcal{K}(x_1, t)\mathrm{d}x_1 \to 2\pi\alpha a\rho_o U^2 \equiv \rho_o \Gamma U$. To calculate the lift at intermediate times to first order in α we can take $X_2 = \mathcal{R}e\{-\mathrm{i}\sqrt{z^2 - a^2}\}$, $z = x_1 + \mathrm{i}x_2$ in the integrand of (4.2) ([18, Section 6.6). The result (first determined by Wagner [38]) is plotted as the solid curve in Figure 6b.

4.2. THE VORTEX WHISTLE

An open-ended tube with a swirling flow of the kind depicted schematically in Figure 7a is called a 'vortex whistle' [35–37]. Fluid enters circumferentially (on the left) at the closed inlet end at a nominally steady rate. The inlet section of diameter D joins a tube of smaller diameter

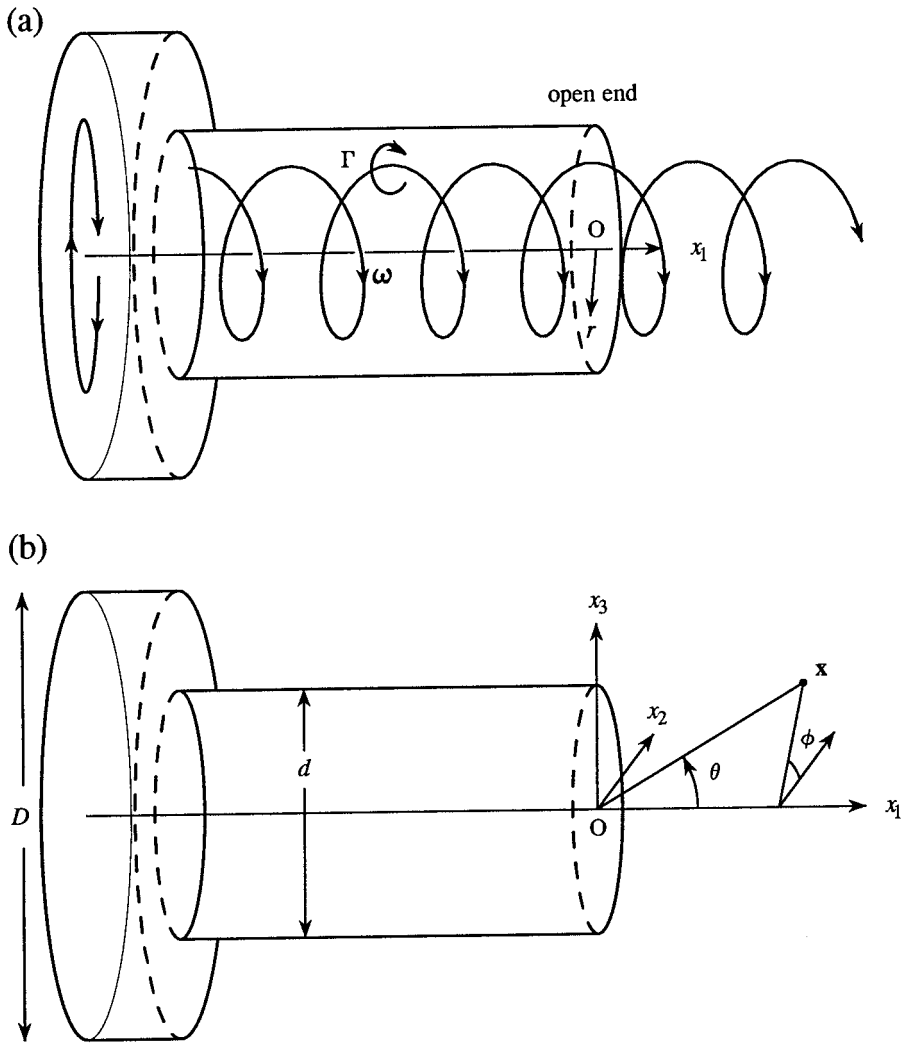

Figure 7. Vortex whistle: (a) unsteady motion driven by an idealized helical vortex; (b) dimensions and coordinate system used to calculate the sound.

$d = 2R$, producing a swirling flow of increased rate of rotation with a nominally axial vortex. Near the open end of the smaller tube the vortex develops quasi-periodic fluctuations, whose interactions with the opening produce aerodynamic sound. According to Vonnegut [35] the frequency of the sound is proportional to the net flow rate through the system, irrespective of whether the working fluid is water or air, and is unrelated to any acoustic or hydrodynamic resonance of the duct.

Observation and numerical simulations [40] indicate that the vortex is displaced from the axis near the open end, where it executes a precessional motion. A simple analytical representation of the production of sound by this motion is obtained by modelling the vortex by the curvilinear helical vortex shown (with schematic exaggeration) in the figure. The vortex strength Γ is equal to the total circulation of the inlet flow in the large section of the duct.

Let the radius of the helix be R_Γ, and let its characteristic wavenumber be κ (> 0) in the mean flow direction (the x_1-direction), so that the pitch is equal to $\Lambda \equiv 2\pi/\kappa$. Take the

coordinate origin at the centre O of the duct exit, with the x_1-axis parallel to the mean exit flow, as indicated in Figure 7. For a suitable choice of the time origin, a point $\mathbf{x}_\Gamma = (x_1, x_2, x_3)$ that lies on the vortex core has the parametric representation in terms of x_1 and t:

$$\mathbf{x}_\Gamma = \Big(x_1,\, R_\Gamma \cos\{\kappa(x_1 - Ut)\},\, R_\Gamma \sin\{\kappa(x_1 - Ut)\}\Big), \tag{4.3}$$

where U is the 'convection' velocity of the helix out of the duct. If $s_\perp$ denotes distance measured along a perpendicular to the vortex from $\mathbf{x}_\Gamma(x_1, t)$, the vorticity distribution (in the neighbourhood of the duct exit) can be written

$$\boldsymbol{\omega} = \frac{\Gamma\delta(s_\perp)}{2\pi s_\perp\sqrt{1+\kappa^2 R_\Gamma^2}}\Big(1,\, -\kappa R_\Gamma \sin\{\kappa(x_1 - Ut)\},\, \kappa R_\Gamma \cos\{\kappa(x_1 - Ut)\}\Big). \tag{4.4}$$

The motion within the duct can be regarded as incompressible, and the sound produced by the interaction of the vortex with the duct exit is determined by the solution (2.29) of the low-Mach-number vortex sound equation (2.26). The compact Green's function can be taken in the form (2.31) when the observer at $\mathbf{x}$ is many acoustic wavelengths from the open end and the source point $\mathbf{y}$ is near the exit. The ideal potential flows represented by the components Y_i of the Kirchhoff vector tend rapidly to zero within the duct. In fact $Y_1 \sim O\Big(\mathrm{e}^{-\alpha|y_1|/R}\Big)$ and $Y_2,\ Y_3 \sim O\Big(\mathrm{e}^{-\beta|y_1|/R}\Big)$ for $|y_1| > R$ in the duct, where α ($\sim 3{\cdot}8$) and β ($\sim 1{\cdot}8$) are respectively the first positive zeros of $\mathrm{J}_1(x)$ and $\mathrm{J}_1'(x)$ [41, Section 3.4]. Thus, if viscous forces on the stationary duct wall are ignored, the acoustic pressure becomes (from (2.29))

$$\begin{aligned} p(\mathbf{x}, t) \;&\approx \frac{-x_j}{4\pi c_o|\mathbf{x}|^2}\frac{\partial}{\partial t}\int (\boldsymbol{\omega}\wedge\mathbf{U})(\mathbf{y}, [t])\cdot\frac{\partial Y_j}{\partial \mathbf{y}}(\mathbf{y})\,\mathrm{d}^3\mathbf{y} \\ &= \frac{-\Gamma U\kappa R_\Gamma x_j}{4\pi c_o|\mathbf{x}|^2}\frac{\partial}{\partial t}\int_{-\infty}^{\infty}\frac{\partial Y_j}{\partial r}\Big(y_1,\, R_\Gamma\cos\{\kappa(y_1 - U[t])\},\, R_\Gamma\sin\{\kappa(y_1 - U[t])\}\Big)\mathrm{d}y_1, \\ &\qquad\qquad |\mathbf{x}| \to \infty, \end{aligned} \tag{4.5}$$

where $r = \sqrt{y_2^2 + y_3^2}$ denotes radial distance from the duct axis, $[t] = t - |\mathbf{x}|/c_o$ is the retarded time, and we have used the relation $\mathrm{d}s = \mathrm{d}y_1\sqrt{1+\kappa^2 R_\Gamma^2}$ between y_1 and distance s measured along the helical vortex.

For a circular cylindrical duct $Y_1(\mathbf{y}) \equiv Y_1(y_1, r)$. The $j = 1$ component of (4.5) is therefore independent of t, and makes no contribution to the sound. According to (2.24) this merely means that the unsteady exit flow produces no fluctuations in the *thrust*. For the transverse components ($j = 2,\ 3$)

$$Y_j(\mathbf{y}) = y_j + \frac{y_j R}{r}\int_{-\infty}^{\infty}\hat{Y}(k, r)\mathrm{e}^{\mathrm{i}ky_1}\mathrm{d}k, \quad j = 2,\ 3, \tag{4.6}$$

where [41]

$$\begin{aligned} \hat{Y}(k, r) \;&= \frac{\mathrm{I}_1(|k|r)}{\pi\mathrm{i}(k + \mathrm{i}0)}\sqrt{\frac{-\mathrm{K}_1'(\kappa R)}{2\mathrm{I}_1'(\kappa R)}}\mathrm{e}^{i\Psi(k)}, \quad r < R, \\ \Psi(k) \;&= \frac{1}{2\pi}\int_{-\infty}^{\infty}\log\left(\frac{\xi^2\mathrm{I}_1'(|\xi|R)\mathrm{K}_1'(|\xi|R)}{k^2\mathrm{I}_1'(|k|R)\mathrm{K}_1'(|k|R)}\right)\frac{\mathrm{d}\xi}{\xi - k}. \end{aligned} \tag{4.7}$$

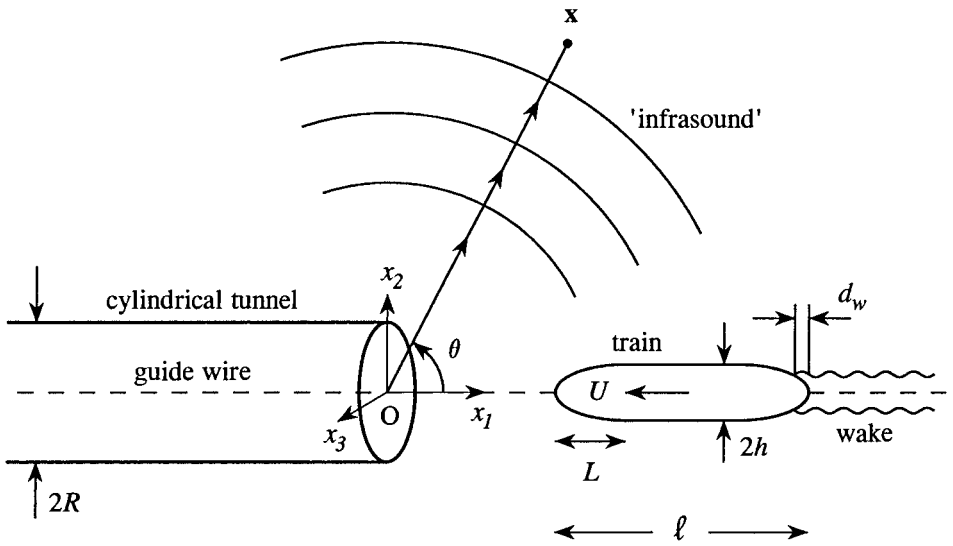

Figure 8. Schematic of experimental axisymmetric model train entering a circular cylindrical tunnel.

In these formulae I_1, K_1 are modified Bessel functions [42, Chapter, 9], and a prime denotes differentiation with respect to the argument.

We now find, from (4.5)

$$p(\mathbf{x},t) \approx \frac{\rho_o U^2 \Gamma(\kappa R)(\kappa R_\Gamma)}{4\pi c_o |\mathbf{x}|} \mathrm{I}_1'(\kappa R_\Gamma) \sqrt{\frac{-2\mathrm{K}_1'(\kappa R)}{\mathrm{I}_1'(\kappa R)}} \sin\theta \cos\{\phi - \Psi(\kappa) + U\kappa[t]\}, \quad |\mathbf{x}| \to \infty, \tag{4.8}$$

where θ and ϕ determine the radiation direction to an observer at $\mathbf{x}$ in the far field, as indicated in Figure 7b. The amplitude of the acoustic pressure $\sim \rho_o U^2 MR/|\mathbf{x}|$, the same as for a compact aerodynamic dipole source. The dipole axis lies in the plane of the open duct exit and rotates about the duct axis at radian frequency $U\kappa$. The dipole strength is equal to the unsteady side force on the duct produced by the 'precessing' vortex close to the exit, as determined by Equation (2.24). The directivity therefore exhibits nulls in the directions $\theta = 0°$ and $180°$ parallel to the jet axis, in agreement with Chanaud's [36] observations.

The dominant frequency of the sound satisfies

$$f = \frac{\omega}{2\pi} = \frac{U}{\Lambda} \sim \frac{U_\mathrm{I}}{\pi D},$$

where U_I is the circumferential, mean flow inlet velocity at the closed end of the duct. Continuity requires the order of magnitude of the *Strouhal* number to be

$$\frac{fd}{U} \sim \frac{1}{\pi} \frac{D^2}{\delta^2} \frac{d}{D}, \quad d = 2R,$$

where δ is the diameter of the inlet pipe. The whistle frequency must therefore increase approximately linearly with the mean flow speed. This is also observed experimentally [35, 37], and confirms the view that the production of sound is not caused by hydrodynamic or acoustic feedback in the duct.

4.3. LOW-FREQUENCY SOUND GENERATED BY A HIGH-SPEED TRAIN ENTERING A TUNNEL

A high-speed train entering a tunnel generates inaudible low-frequency pressure fluctuations (*infrasound*) that cause vibrations and 'rattles' in neighbouring buildings. This important environmental problem involves the generation of sound by the combined actions of a rapidly moving surface and vorticity. Figure 8 illustrates schematically how this is studied experimentally. A scale model 'train' enters a tunnel in the form of a long, rigid circular cylindrical duct. The train is an axisymmetric solid of total length ℓ, and consists of a circular cylindrical mid-section of radius h and cross-sectional area $\mathcal{A}_0 = \pi h^2$, fitted with ellipsoidal nose and tail pieces each of length L. It is projected into the tunnel at speeds of up to 400kph, guided by a tightly stretched steel wire extending along the centre-line of the tunnel and passing through a smooth cylindrical hole drilled along the train axis [43].

Let the tunnel have cross-sectional area $\mathcal{A} = \pi R^2$, and suppose the train travels at constant speed U in the negative x_1-direction, where the origin O is at the center of the tunnel entrance plane. The aspect ratio of the train nose h/L is taken to be sufficiently small, and the train profile sufficiently streamlined, to ensure that flow separation does not occur except in the wake indicated in the figure. In applications the Mach number $M = U/c_o$ does not usually exceed $0\cdot 4$, and the *blockage* $\mathcal{A}_o/\mathcal{A}$ is less than about $0{\cdot}2$.

Introduce a control surface S: $f(x+Ut, y, z) = 0$ that just encloses the moving train (with $f < 0$ inside S and $f > 0$ in the exterior region). When heat transfer and frictional losses are neglected the production of sound is governed by the vortex sound equation (1.8). Multiply this equation by $\mathrm{H} \equiv \mathrm{H}(f)$ and recall that $Df/Dt = 0$ to obtain

$$\left(\frac{\mathrm{D}}{\mathrm{D}t}\left(\frac{1}{c^2}\frac{\mathrm{D}}{\mathrm{D}t}\right) - \frac{1}{\rho}\nabla\cdot(\rho\nabla)\right)(\mathrm{H}B) = \frac{1}{\rho}\mathrm{div}(\mathrm{H}\rho\boldsymbol{\omega}\wedge\mathbf{v}) + \frac{\partial\mathbf{v}}{\partial t}\cdot\nabla\mathrm{H} - \frac{1}{\rho}\mathrm{div}\left(\rho B\nabla\mathrm{H}\right). \quad (4.9)$$

This is analogous to the Ffowcs Williams - Hawkings Equation (2.5); the two terms on the right-hand side involving $\nabla\mathrm{H}$ respectively represent monopole and dipole sources distributed over the surface of the moving train.

We shall approximate the sources by neglecting the compressibility of the air over S. We shall also discard the surface dipoles, which turn out to be second order quantities [44]. Then neglecting nonlinear effects of acoustic *propagation* (4.9) becomes

$$\left(\frac{1}{c_0^2}\frac{\partial^2}{\partial t^2} - \nabla^2\right)(\mathrm{H}B) = \frac{\partial}{\partial t}(\mathbf{U}\cdot\nabla\mathrm{H}) + \mathrm{div}(\mathrm{H}\boldsymbol{\omega}\wedge\mathbf{v}), \quad (4.10)$$

where $\mathbf{U} = (-U, 0, 0)$. The first term is a monopole representing the gross displacement of air by the advancing surface of the train; the vortex source is important principally in the wake of the train.

The wavelength of the sound generated when the train enters the tunnel $\sim O(R/M) \gg R$ for low subsonic train Mach number $M = U/c_o$. Therefore, to solve Equation (4.10) for the acoustic pressure $p \approx B/\rho_o$ outside the tunnel at large distances from the entrance, we can use the following modification of the usual compact Green's function (2.30) for sources close to the entrance ([9], p. 169)

$$\mathcal{G}(\mathbf{x}, \mathbf{y}, t-\tau) = \frac{1}{4\pi\,|\mathbf{X}-\mathbf{Y}|}\delta\left(t - \tau - \frac{|\mathbf{X}-\mathbf{Y}| - (\bar{X}+\bar{Y})}{c_o}\right). \quad (4.11)$$

In this formula $\mathbf{X}(\mathbf{x})$, $\mathbf{Y}(\mathbf{y})$ are defined exactly as for the vortex whistle of Section 4.2, *viz.* the Kirchhoff vector whose i-component is the velocity potential of flow past the stationary surface formed by the tunnel entrance having unit speed in the i-direction at large distances from the entrance (and becoming exponentially small with distance $|x_1|$ *into* the tunnel). The additional terms $\bar{X}$, $\bar{Y}$ determine the *monopole* component of sound generated when an aerodynamic source near the tunnel entrance causes an unsteady volume flux from the tunnel, which can occur for long tunnels because the source compresses the air in the tunnel mouth and produces a sound wave that radiates *into* the tunnel. They are velocity potentials of incompressible flow *out of the tunnel mouth* normalized such that

$$\bar{X}(\mathbf{x}) \sim \begin{cases} x_1 - \ell', & \text{for } |x_1| \gg R \text{ inside the tunnel,} \\ -\mathcal{A}/4\pi|\mathbf{x}|, & \text{for } |\mathbf{x}| \gg R \text{ outside the tunnel.} \end{cases}$$

where $\ell' \approx 0{\cdot}61R$ is Rayleigh's 'end-correction' for an unflanged opening of radius R [45]. Note also that $X_1(\mathbf{x}) = x_1 - \bar{X}(\mathbf{x})$.

In the model scale experiments the aspect ratio $h/L \approx 0{\cdot}3$, which is small enough for the monopole distribution on the right of (4.10) to be approximated by the slender body formula [46]

$$\frac{\partial}{\partial t}\,(\mathbf{U}\cdot\nabla \mathrm{H})\,(\mathbf{x},t) \approx \frac{\partial}{\partial t}\left(U\frac{\partial \mathcal{A}_\mathrm{T}}{\partial x_1}(x_1+Ut)\delta(x_2)\delta(x_3)\right), \tag{4.12}$$

where $\mathcal{A}_\mathrm{T}(s)$ is the cross-sectional area of the train at distance s *from the tip of the nose*, which is assumed to cross the tunnel entrance plane at $t = 0$. This approximation replaces the monopole distribution by a line source along the centreline of the model train. The source strength is proportional to the rate at which the train cross-section changes along the train, and is non-zero only within the profiled nose and tail sections. A train with an ellipsoidal nose profile is obtained by rotating the curve $x_2 = h\sqrt{(x_1/L)(2-x_1/L)}$, $0 < x_1 < L$ about the x_1-axis. Then, similarly, a train of overall length ℓ with identical ellipsoidal nose and tail profiles is specified by

$$\frac{\mathcal{A}_\mathrm{T}(s)}{\mathcal{A}_o} = \begin{cases} \dfrac{s}{L}\left(2-\dfrac{s}{L}\right), & 0 < s < L, \\ 1, & L < s < \ell - L, \\ \left(\dfrac{\ell}{L}-\dfrac{s}{L}\right)\left(2-\dfrac{\ell}{L}+\dfrac{s}{L}\right), & \ell - L < s < \ell. \end{cases} \tag{4.13}$$

In the experiments [43]

$$h = 2{\cdot}135\text{cm}, \quad L = 6{\cdot}3\text{cm}, \quad \ell = 50\text{cm},$$

and the tunnel has radius $R = 5$cm (so that the blockage $\mathcal{A}_o/\mathcal{A} \approx 0{\cdot}18$).

The sound is produced when either the front or tail of the train is close to the entrance. When $|\mathbf{x}| \to \infty$ (in the acoustic far field) Green's function (4.11) can therefore be expanded as a function of the retarded-time variation for source positions $\mathbf{y}$ close to the tunnel entrance. Because the source terms in (4.10) are axisymmetric the first nontrivial term in the expansion is

$$\mathcal{G} \approx \frac{\left\{y_1\cos\theta + (1-\cos\theta)\bar{Y}(\mathbf{y})\right\}}{4\pi c_o|\mathbf{x}|}\,\delta'\left(t-\tau-\frac{|\mathbf{x}|}{c_o}\right), \tag{4.14}$$

where θ is the angle indicated in Figure 8 between the radiation direction $\mathbf{x}$ and the positive x_1-axis. The 'free field' component involving $y_1\cos\theta$ makes no contribution to the acoustic pressure $p_m(\mathbf{x},t)$, say, produced by the monopole (4.12), because

$$\begin{aligned} p_m(\mathbf{x},t) \;&\approx \frac{\rho_o M}{4\pi|\mathbf{x}|}\frac{\partial^2}{\partial t^2}\int\left\{y_1\cos\theta+(1-\cos\theta)\bar{Y}(\mathbf{y})\right\} \\ &\qquad\times\frac{\partial \mathcal{A}_{\mathrm{T}}}{\partial y_1}(y_1+U\tau)\delta(y_2)\delta(y_3)\delta\left(t-\tau-\frac{|\mathbf{x}|}{c_o}\right)\mathrm{d}^3\mathbf{y}\mathrm{d}\tau \\ &= \frac{\rho_o U^2 M(1-\cos\theta)}{4\pi|\mathbf{x}|}\int_{-\infty}^{\infty}\frac{\partial^2\bar{Y}}{\partial y_1^2}(y_1,0,0)\frac{\partial \mathcal{A}_{\mathrm{T}}}{\partial y_1}(y_1+U[t])\,\mathrm{d}y_1, \quad |\mathbf{x}|\to\infty, \end{aligned} \tag{4.15}$$

where $[t]=t-|\mathbf{x}|/c_o$. This integral (which actually extends only over the retarded positions of the nose and tail of the train) must be evaluated numerically, using the following formulae from [46]

$$\begin{aligned} \tfrac{\partial^2\bar{Y}}{\partial y_1^2}(\mathbf{y}) \;&= \frac{-1}{2\pi R}\int_0^\infty \xi\left(\frac{2\mathrm{K}_1(\xi)}{\mathrm{I}_1(\xi)}\right)^{\frac{1}{2}}\cos\left\{\xi\left(\frac{y_1}{R}+\mathcal{Z}(\xi)\right)\right\}\mathrm{d}\xi, \\ \mathcal{Z}(\xi) \;&= \frac{1}{\pi}\int_0^\infty \log\left(\frac{\mathrm{K}_1(\mu)\mathrm{I}_1(\mu)}{\mathrm{K}_1(\xi)\mathrm{I}_1(\xi)}\right)\frac{\mathrm{d}\mu}{\mu^2-\xi^2}. \end{aligned} \tag{4.16}$$

Typical predictions of $p_m(|\mathbf{x}|,\theta,t)$ are displayed in Figures 9b and 9c (dotted curves) for a train entering the tunnel at $U=102$ m/s ($\sim$ 365 kph, $M\sim 0{\cdot}3$). The pressure is plotted as a function of the nondimensional retarded *position* $U[t]/R$ of the train nose respectively for (i) $|\mathbf{x}|=10R\equiv 50\,\mathrm{cm},\ \theta=90^\circ$, (ii) $|\mathbf{x}|=10\sqrt{2}R\equiv 70{\cdot}7\,\mathrm{cm},\ \theta=135^\circ$. The open triangles are the measured pressures at the corresponding points marked (i) and (ii) in Figure 9a. Figure 9a also illustrates the linear pressure directivity pattern ($1-\cos\theta\equiv 2\sin^2(\theta/2)$), which exhibits a strong peak in the 'forward' direction outside the tunnel. The calculated pressures in Figure 9c therefore exceed those in Figure 9b at corresponding retarded times by a factor $\sqrt{2}\sin^2(135^\circ/2)=1{\cdot}207$.

The nose of the train crosses the tunnel entrance plane at $U[t]/R=0$; the train length $\ell=10R$, so that the train is fully within the tunnel for $U[t]/R>10$. The predicted and measured sound begins shortly before nose entry: the first negative pulse represents the sound generated by the nose interacting with the tunnel; its duration $\sim 2R/U$ corresponds to an acoustic pulse of width $\sim 2R/M\approx 7R$. The slightly narrower positive pulse near $U[t]/R=10$ is produced as the tail enters the tunnel. The relatively poor agreement in magnitude near $U[t]/R=0$ at station (i) is believed to be caused by contamination of the measurements by low frequency components of the hydrodynamic or *near* field of the train, which are not accounted for by the acoustic theory [47]. This does not appear to occur at the more distant Station (ii), although much lower frequency disturbances, presumably important at intermediate times, are still evident for $2<U[t]/R<8$.

The monopole source pressure overpredicts the magnitude of the tail-generated pulse, possibly because of the neglect of the wake generated sound. To examine this we model the wake by a circular cylindrical vortex sheet extending axisymmetrically to the rear of the tail (*cf.* Figure 8). The influence of this vorticity on the sound is governed by the vortex source $\mathrm{div}(\mathrm{H}\boldsymbol{\omega}\wedge\mathbf{v})$ in Equation (4.10). However, because of the uncertainty in specifying the vortex strength, and because the wake forms a nominally fixed structure in a frame moving with

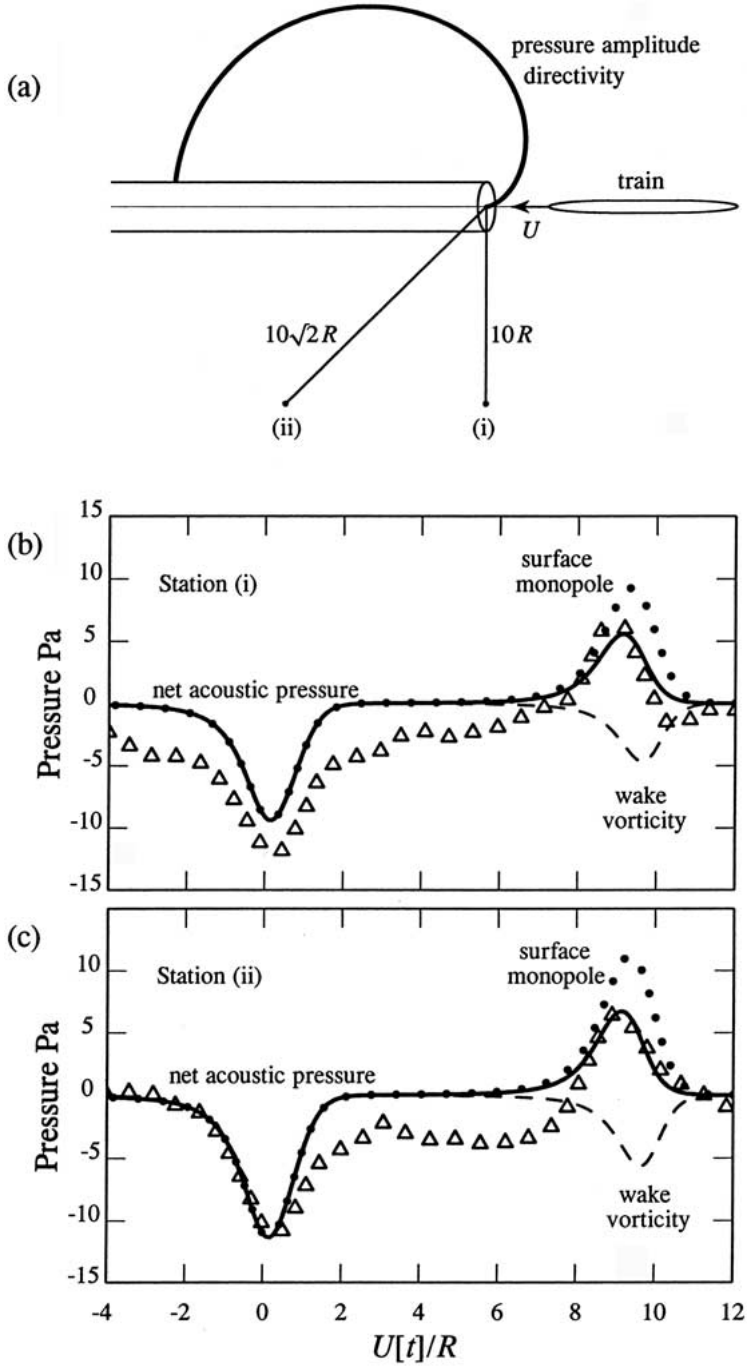

Figure 9. (a) Directivity of the acoustic pressure amplitude; (b), (c) △ △ △, measured pressures at Stations (i) and (ii); —— overall predicted pressure; • • •, monopole pressure p_m; - - - -, wake induced pressure p_w (plotted only for $U[t]/R > 4$).

the train, we can estimate its influence indirectly, by re-defining the moving control surface $f(x + Ut, y, z) = 0$ so that it just encloses the surface of the train *ahead* of the wake *and* the the outer boundary of the wake flow. This surface lies just outside the wake so that $\boldsymbol{\omega} \equiv \mathbf{0}$ in the region $f > 0$. Thus, the influence of the wake is represented by extending the monopole source on the right of (4.10) to include a contribution from the surface of the wake; at the same time the original monopole source distribution (4.12) must be modified to include only that part of the surface of the train upstream of the wake. Now $\mathbf{U} \cdot \nabla \mathrm{H} \equiv 0$ on the wake boundary when the latter is modelled by a circular cylindrical surface whose generators are parallel to the direction of motion of the train, so that the monopole strength actually vanishes on the portion of $f(x + Ut, y, z) = 0$ representing the surface of the wake . The acoustic pressure is therefore given by the following modified form of (4.15)

$$p_m(\mathbf{x}, t) \approx \frac{\rho_o U^2 M(1 - \cos\theta)}{4\pi |\mathbf{x}|} \int_{-\infty}^{\ell - U[t] - d_w} \frac{\partial^2 \bar{Y}}{\partial y_1^2}(y_1, 0, 0) \frac{\partial \mathcal{A}_\mathrm{T}}{\partial y_1}(y_1 + U[t])\, \mathrm{d}y_1, \quad |\mathbf{x}| \to \infty, \tag{4.17}$$

where d_w is the axial distance (indicated in Figure 8) upstream of the end of the train at which the mean flow separates from the profiled tail section, and beyond which the wake is assumed to have the form of a circular cylinder. According to this model, the acoustic pressure p_w, say, associated with the wake vorticity is given by

$$p_w(\mathbf{x}, t) \approx -\frac{\rho_o U^2 M(1 - \cos\theta)}{4\pi |\mathbf{x}|} \int_{\ell - U[t] - d_w}^{\infty} \frac{\partial^2 \bar{Y}}{\partial y_1^2}(y_1, 0, 0) \frac{\partial \mathcal{A}_\mathrm{T}}{\partial y_1}(y_1 + U[t])\, \mathrm{d}y_1, \quad |\mathbf{x}| \to \infty, \tag{4.18}$$

The magnitude of the wake contribution p_w depends on the separation distance d_w. Numerical simulations [48] indicate that $d_w = 0{\cdot}25R \sim 0{\cdot}2L$ is representative of the real situation, and the corresponding predictions for p_w are plotted as the broken line curves in Figure 9. The wake generated sound is significant only as the tail of the train passes into the tunnel, where it produces a negative pulse that opposes the tail monopole, and brings down the overall predicted acoustic pressure to values comparable with the measurements.

5. Conclusion

Lighthill's advocacy of vortex methods extended to most areas of fluid mechanics except aerodynamic sound. In the late 1950's he pioneered the 'vortex method' for the numerical solution of unsteady flow problems; this has since become one of the major tools for investigating complex flow-structure interactions at low Mach numbers. It also provides the most efficient means of calculating the acoustic noise produced by these flows.

The 'acoustic analogy' expresses the equivalence of sound production by a flow and the generation of sound in an ideal, stationary medium driven predominantly by the real-flow-Reynolds-stress fluctuations. In homentropic flows the theory can be recast into a form where vorticity alone may be identified as the ultimate 'source' of sound. For *compact* flow-structure interactions this alternative representation of sound generation is a natural consequence of the classical concept of 'vortex impulse', which Lighthill regarded as sufficiently fundamental to be included in his undergraduate lectures at University College, London. The examples worked out in this paper illustrate how the awkward dependence on bound vorticity in the classical formula for the 'impulse' is removed by the introduction of the 'Kirchhoff vector',

making it suitable for routine numerical or analytical evaluation. Difficulties frequently experienced in the application of the acoustic analogy to non-compact flow-structure interactions are similarly resolved by the methods of vortex sound theory, as exemplified by our treatment of the infrasound generated by a high-speed train entering a tunnel.

References

1. Lord Kelvin, On vortex motion. *Trans. R. Soc. Edinburgh* 25 (1869) 217–260. (also *Collected Works*, Volume IV, 13–65.)
2. M. J. Lighthill. Chapters 1: *Introduction. Real and Ideal Fluids*; and Chapter 2: *Introduction. Boundary Layer Theory*. In: L. Rosenhead (ed.), *Laminar Boundary Layers*. Oxford: Oxford Univ. Press (1963) pp. 1–113.
3. A. J. Chorin, *Vorticity and Turbulence* (corrected edition). New York: Springer-Verlag (1998) 74 pp.
4. G.-H. Cottet and P. D. Koumoutsakos, *Vortex Methods: Theory and Practice*. Cambridge: Cambridge Univ. Press (2000) 313 pp.
5. M. J. Lighthill, On sound generated aerodynamically. Part I: General theory. *Proc. R. Soc. London* A211 (1952) 564–587.
6. J. E. Ffowcs Williams, The noise from turbulence convected at high speed. *Phil Trans R. Soc. London* A255 (1963) 469–503.
7. J. E. Ffowcs Williams and D. L. Hawkings, Sound generation by turbulence and surfaces in arbitrary motion. *Phil. Trans. R. Soc. London* A264 (1969) 321–342.
8. J. E. Ffowcs Williams, Sound production at the edge of a steady flow. *J. Fluid Mech.* 66 (1974) 791–816.
9. M. S. Howe, *Acoustics of Fluid-Structure Interactions*, Cambridge: Cambridge Univ. Press (1998) 560 pp.
10. D. G. Crighton, Basic principles of aerodynamic noise generation. *Prog. Aerosp. Sci.* 16 (1975) 31–96.
11. J. E. Ffowcs Williams, Aeroacoustics. *Ann. Rev. Fluid Mech.* 9 (1977) 447–468.
12. J. O. Hinze, *Turbulence* (Second edition). New York: McGraw-Hill (1975) 90 pp.
13. A. Powell, Theory of Vortex Sound *J. Acoust. Soc. Am.* 36 (1964) 177–195.
14. A. Powell, Private communication (2000).
15. N. Curle, The influence of solid boundaries upon aerodynamic sound. *Proc. R. Soc. London* A231 (1955) 505–514.
16. Sir James Lighthill, *Mathematical Biofluiddynamics*. Philadelphia: Soc. Ind. Appl. Math. (1975) 281 pp.
17. J. Lighthill, *An Informal Introduction to Theoretical Fluid Mechanics*. Oxford: Clarendon Press (1986) 260 pp.
18. G. K. Batchelor, *An Introduction to Fluid Dynamics*. Cambridge: Cambridge Univ. Press (1967) 260 pp.
19. James Lighthill, *Waves in Fluids*. Cambridge: Cambridge Univ. Press (1978).
20. S. C. Crow, Aerodynamic sound emission as a singular perturbation problem. *Studies Appl. Math.* 49 (1970) 21–44.
21. L. D. Landau and E. M. Lifshitz, *Fluid Mechanics* (Second edition). Oxford: Pergamon (1987) 38 pp.
22. D. G. Crighton, A. P. Dowling, J. E. Ffowcs Williams, M. Heckl and F. G. Leppington, *Modern Methods in Analytical Acoustics (Lecture Notes)*. London: Springer-Verlag (1992), 738 pp.
23. W. Möhring, On vortex sound at low Mach number. *J. Fluid Mech.* 85 (1978) 685–691.
24. M. S. Howe, On unsteady surface forces, and sound produced by the normal chopping of a rectilinear vortex. *J. Fluid Mech.* 206 (1989) 131–153.
25. B. B. Baker and E. T. Copson, *The Mathematical Theory of Huygens' Principle*, Second edition. Oxford: Oxford Univ. Press (1969) 192 pp.
26. R. H. Kraichnan, Pressure fluctuations in turbulent flow over a flat plate. *J. Acoust. Soc. Am.* 28 (1956) 378–390.
27. O. M. Phillips, On the aerodynamic surface sound from a plane turbulent boundary layer. *Proc. R. Soc. London* A234 (1956) 327–335.
28. M. S. Howe, A Note on the Kraichnan-Phillips theorem. *J. Fluid Mech.* 234 (1992) 443–448.
29. A. Powell, Aerodynamic noise and the plane boundary. *J. Acoust. Soc. Am.* 32 (1960) 962–990.
30. J. E. Ffowcs Williams, Sound radiation from turbulent boundary layers formed on compliant surfaces. *J. Fluid Mech.* 22 (1965) 347–358.
31. J. E. Ffowcs Williams and L. H. Hall, Aerodynamic sound generation by turbulent flow in the vicinity of a scattering half-plane. *J. Fluid Mech.* 40 (1970) 657–670.

32. M. S. Howe, Trailing edge noise at low Mach numbers. *J. Sound Vibr.* 225 (1999) 211–238.
33. M. J. Lighthill, *An Introduction to Fourier Analysis and Generalised Functions*, Cambridge Univ. Press (1958) 79 pp.
34. M. S. Howe, *Reference Manual on the Theory of Lifting Surface Noise at Low Mach Numbers*. Boston University, Department of Aerospace and Mechanical Engineering Report AM-98-001 (1998).
35. B. Vonnegut, A vortex whistle. *J. Acoust. Soc. Am.* 26 (1954) 18–20.
36. R. C. Chanaud, Experiments concerning the vortex whistle. *J. Acoust. Soc. Am.* 35 (1963) 953–960.
37. R. C. Chanaud, Observations of oscillatory motion in certain swirling flows. *J. Fluid Mech.* 21 (1965) 111–127.
38. H. Wagner, Über die Einstehung des dynamischen Auftriebes von Tragflügeln. *Zeitschrift für angewandte Mathematik und Mechanik* 5 (1925) 17–35.
39. P. G. Saffman, *Vortex Dynamics*. Cambridge: Cambridge Univ. Press (1993) 311 pp.
40. S. Kaji, H. Kobayashi and S. Momo, Simulation of sound generation in a vortex whistle. Paper presented at the *7th International Congress on Sound and Vibration*. Garmisch, Germany (July 2000).
41. B. Noble, *Methods Based on the Wiener-Hopf Technique*. London: Pergamon Press (1958) (reprinted 1988, New York: Chelsea Publishing Company) 246 pp.
42. M. Abramowitz and I. A. Stegun (eds.), *Handbook of Mathematical Functions* (Ninth corrected printing), US Department of Commerce, National Bureau of Standards Applied Mathematics Series No.55 (1970) 1046 pp.
43. M. Iida, K. Kikuchi and T. Fukuda, A pressure wave radiated from a tunnel entrance when a train enters a tunnel. Paper presented at the *10th International Symposium on Aerodynamics and Ventilation of Vehicle Tunnels*, Boston, USA: 1–3 November 2000.
44. M. S. Howe, M. Iida, T. Fukuda and T. Maeda, Theoretical and experimental investigation of the compression wave generated by a train entering a tunnel with a flared portal *J. Fluid Mech.* 425 (2000) 111–132.
45. Lord Rayleigh, *The Theory of Sound*, Volume 2. New York: Dover (1945) 504 pp.
46. M. S. Howe, The compression wave produced by a high-speed train entering a tunnel. *Proc. R. Soc. London* 454 (1998) 1523–1534.
47. M. Iida, Private communication (2000).
48. J. A. Schetz, Aerodynamics of high-speed trains. *Ann. Rev. Fluid Mech.* 33 (2001) 371–414.